



Geology of the Monapo Klippe, NE Mozambique and its significance for assembly of central Gondwana

P.H. Macey^a, J.A. Miller^{b,*}, C.D. Rowe^{c,1}, G.H. Grantham^d, P. Siegfried^e, R.A. Armstrong^f, J. Kemp^g, J. Bacalau^h

^a Western Cape Unit, Council for Geoscience, PO Box 572, Bellville 7530, South Africa

^b Department of Earth Sciences, Stellenbosch University, Private Bag X1, Matieland 7602, South Africa

^c Department of Geological Sciences, University of Cape Town, Private Bag X3, Rondebosch 7701, South Africa

^d Central Regions Unit, Council for Geoscience, Private Bag X112, Pretoria 0001, South Africa

^e GeoAfrica Prospecting Services cc, PO Box 24218, Windhoek, Namibia

^f Research School of Earth Sciences, Australian National University, Canberra, Australia

^g Department of Geography and Environmental Studies, Stellenbosch University, Private Bag X1, Matieland 7602, South Africa

^h National Directorate for Geology, Nampula Regional Office, Mozambique

ARTICLE INFO

Article history:

Received 2 June 2012

Received in revised form 5 February 2013

Accepted 19 March 2013

Available online xxx

Keywords:

Monapo Klippe

Lithostratigraphy

Geochronology

Mozambique

Gondwana assembly

ABSTRACT

The Monapo Klippe in north-east Mozambique is an ovoid-shaped outcrop measuring approximately 35 × 40 km and is clearly visible on satellite and geophysical images. Based on recent field mapping, geochemical studies and new geochronological data, we present a revision of the lithostratigraphy of the klippe and offer a model for its origin and emplacement in the framework of regional tectonics. There are three main groups of rocks within the klippe: (1) the Metachéria Metamorphic Complex; (2) the Mazerapane Intrusive Suite; and (3) the Ramiane Intrusive Suite. The Metachéria Metamorphic Complex consists of a mélange of granulite gneiss, including mafic, felsic, pelitic and carbonate rocks, characterised by a strong penetrative shear fabric. The largely undeformed Mazerapane and Ramiane Suites have intruded into the Metachéria Metamorphic Complex. The Mazerapane Suite consists of foid-bearing ultramafic and mafic gneisses and intrudes into the western half of the complex, whereas the Ramiane Suite is dominated by alkaline granitic rocks, contains no foid-bearing units and intrudes into the eastern half of the complex. In addition to these three main units, there are a number of minor but structurally important units, the main ones of which include amphibolite-facies tonalitic gneisses and the Evate calcite carbonatite. Underlying all of these units is a narrow, high strain mylonite zone. Undeformed pegmatite bodies and dykes cross-cut all rock types of the Monapo Klippe including the marginal mylonite. Near identical dates for the intrusion of the Ramiane Suite at 637 ± 5 Ma and metamorphism of the Metachéria Complex at 634 ± 8 Ma indicates a major episode of granulite-facies metamorphism and crust generation at this time. The ~ 635 Ma age for the granulite-facies metamorphism is comparable to granulite-facies events identified in other parts of the East African Orogen in Tanzania, Madagascar and other parts of northern Mozambique to the north of the Lúrio Belt. The absence of granulite-facies rocks in the underlying Nampula Block is consistent with structural arguments that the Monapo Klippe is the remnant of an allochthonous thrust sheet. In this context, the Monapo Complex is very similar to other granulite-facies "klippe" in East Africa, Antarctica and Sri Lanka, lending support to the idea of a Pan-African mega-nappe formerly existing across greater East Gondwanaland.

© 2013 Elsevier B.V. All rights reserved.

1. Introduction

The diverse terranes amalgamated during the Meso to Neoproterozoic to form present day northern Mozambique preserve

a record of the kinematics of Gondwana construction as well as an opportunity to observe deeper crustal levels of a large orogenic belt. The crust in northern Mozambique is cut into two similar but different tectonic blocks by the ENE-trending, NW-dipping Lúrio Belt. This belt is made up of highly strained Neoproterozoic mafic granulites of the Ocua Complex and is thought to mark a major crustal boundary (Fig. 1; Viola et al., 2008; Bingen et al., 2009; Macey et al., 2010). To the south of the Lúrio Belt, the Nampula Block (the Nampula Complex of Jacobs et al., 2008) forms a large contiguous crustal block which consists of 1150–1070 Ma orthogneisses and

* Corresponding author. Tel.: +27 218083121; fax: +27 218083129.

E-mail address: jmiller@sun.ac.za (J.A. Miller).

¹ Present address: Department of Earth and Planetary Sciences, McGill University, 3450 University Street, Montréal, QC H3A 0E8, Canada.

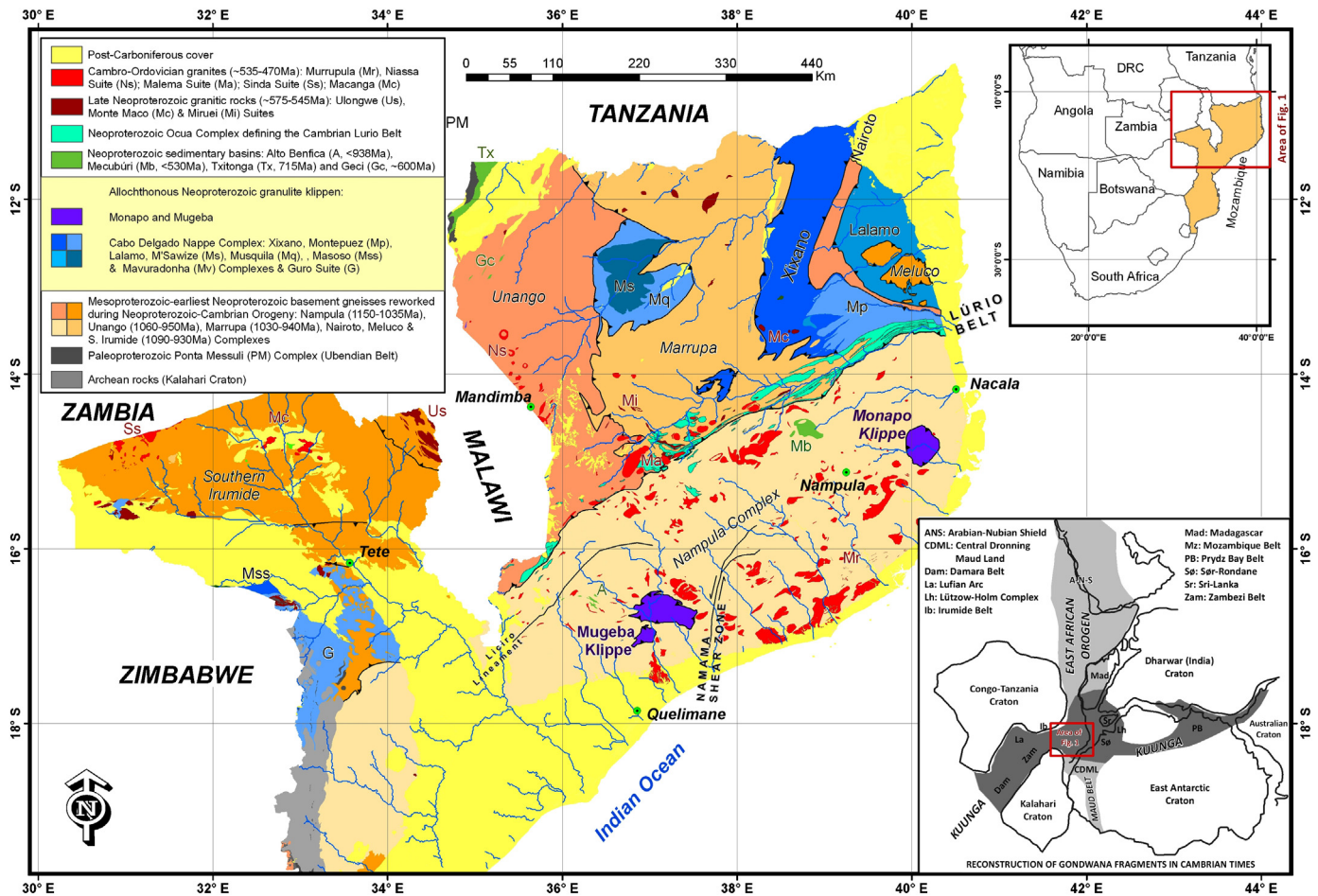


Fig. 1. Simplified geological map of NE Mozambique after Norconsult (2007a,b), Macey et al. (2007) and Grantham et al. (2007) showing the main lithostratigraphic units. Bottom inset shows reconstruction of Gondwana during the Cambrian after Meert (2003), with the locations of the East African Orogen and Kuunga Orogen shown.

metasedimentary rocks with high grade metamorphism around 1090–1070 Ma (Macey et al., 2010). The Mesoproterozoic rocks of the Nampula Block are overlain by isolated allochthonous Neoproterozoic granulite klippen (Monapo and Mugeba Klippen; Pinna et al., 1993; Grantham et al., 2008) and para-autochthonous metamorphosed molasse sediments (Mecubúri and Alto Benfica Groups; Thomas et al., 2010; Fig. 1). The Namuno Block (Grantham et al., 2008) north of the Lúrio Belt consists of similar Mesoproterozoic crustal gneisses (Unango and Marrupa Complexes), but with slightly younger protolith ages, 1060–940 Ma (Bingen et al., 2009), and metamorphic ages ~940 Ma that are interleaved with slices of high grade metamorphic rocks of more mafic character, the Neoproterozoic Cabo Delgado Nappe Complex (including the Xixano, M'Sawize, Muaquia and Lalamo complexes), forming a stack of west vergent, nappes (Viola et al., 2008; Bingen et al., 2009; Boyd et al., 2010). The various litho-tectonic entities were tectonically juxtaposed during the protracted, late Neoproterozoic to early Paleozoic (c. 630–495 Ma) amalgamation of Gondwana (e.g. Jacobs et al., 1998, 2008; Meert, 2003; Stern, 2004; Collins and Pisarevsky, 2005; Collins et al., 2007; Grantham et al., 2008; Bingen et al., 2009). Collisional orogenesis was followed by the intrusion of late- to post tectonic Cambrian-Ordovician K-granites, in particular the voluminous Murrupula Suite (~530–495 Ma) that intrudes the Nampula Block (Macey et al., 2007; Jacobs et al., 2008; Ueda et al., 2012).

Two principal models have been proposed to explain the current architecture and geological evolution of Northern Mozambique crust, and in particular, the nature of the Lúrio Belt. In the first model, assembly involves convergence of eastern and western

Gondwana associated with closure of the Mozambique Ocean along the East African Orogen (Holmes, 1951; Stern, 2004) extending southward into Antarctica to form the East African Antarctic Orogen (EAAO) (Jacobs and Thomas, 2004; Jacobs et al., 2008). In this model the Lúrio Belt of Northern Mozambique represents an accommodation zone between two thermomechanically very different parts of the EAAO, separating a part where the orogen root delaminated from a part that did not delaminate (Jacobs et al., 2008) and as such it does not represent a Neoproterozoic suture zone (Jacobs and Thomas, 2004; Jacobs et al., 2008). The Mecubúri and Alto Benfica Groups were deposited in basins that developed as a result of extensional collapse of the thickened lithosphere of the EAAO, near-contemporaneous with the intrusion of post-collisional granites into the Nampula Block (Jacobs et al., 2008; Thomas et al., 2010; Ueda et al., 2012).

The second model proposes a two-stage amalgamation of Gondwana components (Grantham et al., 2008, in press). The first stage involves the collision between east and west Gondwana components (the microcontinent Azania colliding with the Congo-Tanzania-Bangweulu block; Collins and Pisarevsky, 2005) forming the N-S trending East African Orogen (750–620 Ma; Stern, 1994; Meert, 2003) and, in northern Mozambique, formation of the west-vergent Namuno accretionary terrane stack. The second stage involves the collision of the newly formed this northern Gondwana block (combined East African Orogen, Namuno Block) with a southern Gondwana block (Nampula-Kalahari-western Dronning Maud Land) along the E-W striking Damara-Lufilian-Zambezi-Lúrio-Prydz Bay belts alternatively referred to as the Malagasy

Orogeny (550–520 Ma) west of India (Collins and Pisarevsky, 2005) and the Kuunga Orogeny (570–530 Ma) to the east of India where it also involves the collision of the Australia and Mawson Blocks (Boger et al., 2001; Meert, 2003; Fig. 1). The transpressional collision resulted in thrusting of northern Gondwana (Namuno Block) over southern Gondwana (Nampula Block) along the Lúrio Belt. As the orogen grew, the Mecubúri and Alto Benfica Groups were deposited as molasse into foreland basins developed in the Nampula Block ahead of the advancing thrust front with detritus derived from the Namuno Block. The sediments were subsequently rapidly buried and metamorphosed to medium- to high grades by the overriding Namuno Block roughly synchronous with the intrusion of the earliest K-granites into the footwall gneisses of the Nampula Block (Grantham et al., in press).

Grantham et al. (2008) and Grantham et al. (in press) regard the Monapo and Mugeba klippen overlying the Nampula Block to represent erosional remnants of the Namuno Block nappe and, more specifically, the Cabo Delgado granulite complex. Gondwana reconstructions place Dronning Maud Land, Antarctica and Sri Lanka adjacent to Northern Mozambique, and Grantham et al. (2008) propose that other klippe such as the Sør Rondane in Dronning Maud Land, Kartaragama in Sri Lanka and the Urungwe in Zimbabwe may also represent remnants of the once sub-continental scale thrust sheet.

Recent geological mapping and research across Northern Mozambique and its Gondwana neighbours has greatly improved our understanding of many of the Mesoproterozoic tectonic blocks (e.g. Sacchi et al., 1984, 2000; Pinna et al., 1993; Kriegsman, 1995; Kröner et al., 1997; Kröner et al., 2001; Macey et al., 2007, 2010; Grantham et al., 2007, 2008; Jacobs et al., 2003, 2008; Viola et al., 2008; Bingen et al., 2009; Boyd et al., 2010; Ueda et al., 2012) but data for the smaller, poorly outcropping Neoproterozoic granulitic nappe complexes is comparatively limited (Pinna et al., 1993; Engvik et al., 2007). What is known is that granulite-facies metamorphism in all of these complexes generally spans the time frame 735–550 Ma with distinct peaks at 640 Ma and 590 Ma (Kröner et al., 1997; Norconsult, 2007a,b; Grantham et al., 2007, in press; Macey et al., 2007, 2010; Bingen et al., 2009; Boyd et al., 2010). P-T conditions associated with this event vary spatially but are estimated to span the range 700–800 °C and 7–8.5 kbar up to 910 ± 20 °C at 9–11.5 kbar (Roberts et al., 2005; Jamal, 2005; Engvik et al., 2007; Grantham et al., in press). Since the correlation of these granulite-facies remnants has underpinned the concept of a regionally extensive granulitic-facies mega-nappe sheet developing during Gondwana assembly, a detailed understanding their stratigraphic, geochronological and tectono-metamorphic evolution is key to testing the Namuno nappe model. In this study we present a new geologic framework for the Monapo Klippe, integrating field observations with petrographic, geochemical, and geochronologic data with the aim of clarifying the origin of the Monapo structure and placing it within the regional tectonic framework for central Gondwana. We discuss the relationship of the Monapo structure to the granulite-facies Cabo Delgado Nappes of northern Mozambique (Viola et al., 2008) as well as its correlation to other granulite-facies remnants within Tanzania, Sri Lanka, Antarctica and Madagascar (Hölzl et al., 1994; Muhongo et al., 2001; Muhongo and Lenoir, 1994; Ravikant, 2006; Sajeev et al., 2007; Ravikant et al., 2008; Jöns and Schenk, 2008; Grantham et al., in press).

2. Geology of the Nampula Block

The Monapo and Mugeba klippen preserve lithological assemblages, metamorphic conditions and structural histories that are unlike the surrounding Nampula gneisses (Macey et al., 2010).

In order to demonstrate these differences, this section provides a short summary of the geology of the underlying Nampula Block. The Nampula Block is made up of five Mesoproterozoic ortho- and paragneiss suites with largely uniform tectonic histories (Grantham et al., 2007; Macey et al., 2007; Bingen et al., 2009; Macey et al., 2010). The five main groups of Mesoproterozoic rocks are the Mocuba Complex (meta-TTG orthogneisses, c. 1125 Ma), Rapale Gneiss (meta-tonalite orthogneiss, c. 1095 Ma), Mamala Gneiss (quartz-feldspathic gneiss; c. 1090 Ma), Molòqué Complex (meta-sedimentary rocks; <1125 Ma) and Culicui Suite (granitoid orthogneiss; c. 1075 Ma) (Macey et al., 2010). The Mocuba and Rapale Gneisses have low-K signatures and probably represent one or more juvenile TTG-type calc-alkaline volcanic arc complexes, which formed, amalgamated and accreted to the Kalahari Craton during the Mesoproterozoic. The Mocuba Gneisses have experienced several phases of deformation and contain evidence for an early D₁ deformation event (intrafolial folds, refolded leucosomes). The absence of evidence for this event in the slightly younger Rapale Gneiss, suggests that this event predates 1095 Ma. The Culicui Gneisses have variable but higher-K signatures suggesting the evolution to a more mature arc-setting by 1075 Ma.

In addition to the allochthonous Monapo and Mugeba klippen, the Mesoproterozoic rocks of the Nampula Block are unconformably overlain by the Neoproterozoic meta-sedimentary rocks (conglomerates, arenites and pelites) of the Mecubúri and Alto Benfica Groups (Thomas et al., 2010; Fig. 1). Dating of detrital zircons from the Mecubúri Group indicate source rocks with ages peaking between ~1100–950 Ma, 750–800 Ma and 700–530 Ma, similar to the crystallisation ages in the Namuno Block. The youngest zircon provides a maximum depositional age of 530 Ma. The Nampula Block does not contain any rocks aged between ~1000 and 600 Ma indicating that the Mecubúri Group was deposited onto the Nampula Block at ~530 Ma with much of the detritus coming from the Namuno Block.

Deformation during the Neoproterozoic and Cambrian times resulted in a regional penetrative gneissosity that transposes all earlier Mesoproterozoic fabrics. Peak regional metamorphism was typically mid- to upper-amphibolite facies with P-T conditions estimated at 700 °C and 7–8 kbar. Metamorphic zircon and monazite were dated between ~550 and 500 Ma (Bingen et al., 2009; Macey et al., 2010; Thomas et al., 2010; Grantham et al., in press).

The Nampula Block is intruded by weakly to undeformed Cambrian granites of the Murrupula Suite. The oldest of the Murrupula Suite granitoids, the weakly deformed porphyritic Mopui quartz monzonite, yielded a zircon U-Pb Concordia crystallisation age of 532 ± 4.6 Ma (Macey et al., 2007). Six undeformed equigranular granite plutons gave crystallisation ages ranging from 514 to 504 Ma (zircon U-Pb SHRIMP; Macey et al., 2007). These Cambrian granites do not appear to have intruded into the Monapo Klippe and it is unknown if they intrude into the Mugeba structure. At least two generations of pegmatites intruded the rocks of the Nampula Block. The weak to moderately deformed pegmatite phase has been dated at 501 ± 5 Ma using U-Pb SHRIMP dating of zircon (Macey et al., 2007). It is unclear if pegmatites in the Monapo Klippe are related to one of these generations as the metamict state of the zircons has not allowed them to be dated as yet.

3. Delineation of the Monapo Klippe

The Monapo Klippe is an ovoid-shaped structure measuring approximately 35×40 km that is clearly visible on aeromagnetic, aeroradiometric and Landsat 7 images (Fig. 2). Despite this, the outcrop in the field is generally poor, with some units having reasonable outcrop but others almost none at all. In particular the boundaries of the Monapo Klippe have been difficult to define

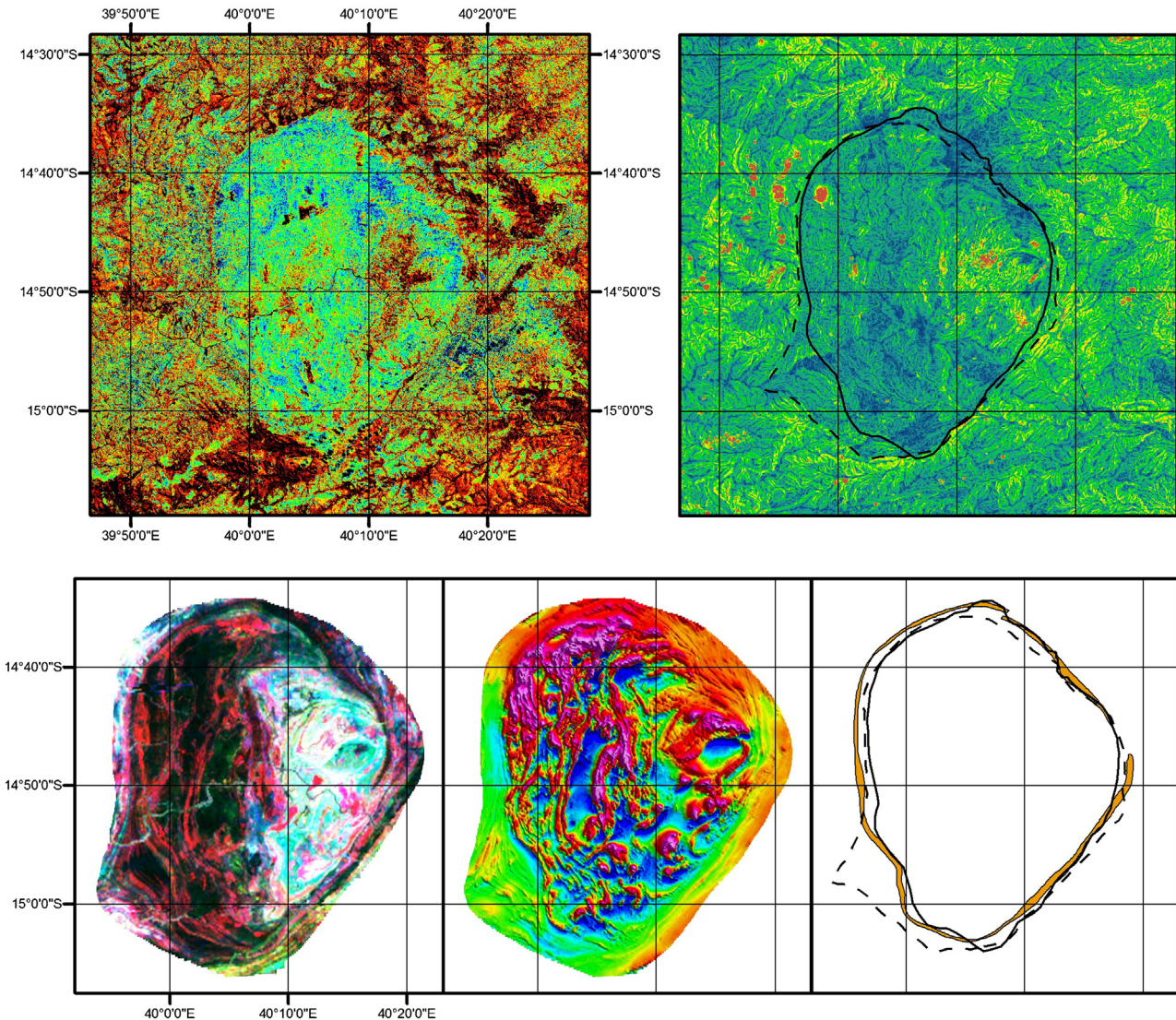


Fig. 2. Geophysical, radiometric and landsat imagery of the Monapo Klippe. (a) Landsat 7 Principal Components Analysis (PC2); (b) topographic slope from SRTM DEM; (c) ternary Radiometrics; (d) aeromagnetics; (e) outlines of the Monapo Klippe: dotted line—outline digitised from slope, solid line: outline digitised from Landsat PCA, outline of mapped marginal mylonite.

because of the extremely poor nature of the exposure of the rocks making up the marginal mylonite (see below). This is compounded by the generally low topographic relief of the klippe. Previous maps show a prominent bulge in the south-west margin of the Monapo (BULGAROEOMIN, 1984) and the rocks there are defined as biotite or biotite + amphibole gneisses with garnet + clinopyroxene-bearing bands and amphibole + pyroxene-bearing marbles. In the revised map of Siegfried (1999), this bulge has been replaced by a series of thrust faults with the edge of the marginal mylonite drawn much closer in. In the map produced by Grantham et al. (2007) as part of the World Bank Project, the boundary of the Monapo Klippe has again been extended into the bulge region of BULGAROEOMIN (1984) but the rocks have been reassigned to the marginal mylonite unit making this unit fairly wide in the south-west. This is based in part on interpretation of geophysical and radiometric data which shows prominent curvilinear features in this region (Fig. 2c and d). However, aeromagnetics indicates that these features are outside the Monapo (Fig. 2d) whereas ternary U-Th-K radiometrics suggests that they are inside the Monapo (Fig. 2c). Principal component analysis performed on Landsat 7 ETM+ imagery (Fig. 2a and b) in combination with field observations indicates that these lines

are likely to be thrust slices in basement rocks that are more prominently exposed because of the orientation of topographic drainage in this region (Fig. 2b). These thrust slices are most likely related to emplacement of the Monapo Klippe but are sheared and thrusted Nampula footwall rocks of the Monapo. Hence the boundary of the Monapo Klippe has been aligned with known field exposures of the marginal mylonite and the well-defined boundary shown in Fig. 2f (total aeromagnetics, ternary U-Th-K, Landsat).

4. Rock types of the Monapo Klippe

At least two previous stratigraphic subdivisions (Table 1) have been proposed for the Monapo Klippe (Jourde et al., 1974; BULGAROEOMIN, 1984; Pinna and Marteau, 1987; Pinna et al., 1993; Lachelt, 2004). In the earliest stratigraphic subdivision by Jourde et al. (1974), the bulk of the rocks of the Monapo Klippe were assigned to the Monapo Series, and included gabbroic to granitic granulites, anorthosites, marble and sillimanite gneisses, monzonitic gneisses including some silica-undersaturated varieties, syeno-diorites and pyroxenites. This series was intruded by three rock types that included calc-alkaline granite, sub-alkaline

Table 1

Lithodemic units of the Monapo Klippe and previous stratigraphic subdivisions.

THIS STUDY after Macey et al. (2007); Grantham et al. (2007)	PINNA ET AL. (1986) and summarized by Lächelt (2004)	B.R.G.M. Jourde et al. (1974), BULGARGEOMIN (1984)
 RAMIANE SUITE MAZERAPANE SUITE METACHÉRIA METAMORPHIC COMPLEX 	Namiale Metachéria Formation MONAPO GROUP 	ROCHAS INTRUSIVAS NA SÉRIE DO MONAPO SÉRIE DO MONAPO Formação de Namialo Metachéria Formação de Ramiane

syenites and monzonites, all of which were amphibole-bearing. This subdivision was revised by Pinna and Marteau (1987), Pinna et al. (1993) and summarised by Lächelt (2004). In the revision, all the rocks of the Monapo Klippe were assigned to the Monapo Group that formed part of a package of rocks that were called the Lúrio Supergroup (Lächelt, 2004). The Monapo Group was further subdivided into two units: the basal Ramiane (or Evate) Formation, which comprised a range of generally mylonitic rocks (Table 1) and the overlying Namiale-Metachéria Formation (Pinna and Marteau, 1987; Pinna et al., 1993). The Namiale-Metachéria Formation consisted of a range of mafic, ultramafic and silica-undersaturated rocks (Table 1).

There are three main problems with these subdivisions: (1) modern lithostratigraphic classifications do not allow for the terms Supergroup, Group and Formation to be used for high grade metamorphic and plutonic igneous rocks; (2) both formations consist of a wide range of rock types that are clearly genetically unrelated; and (3) the map produced by Jourde et al. (1974) is significantly different to the one presented in this study (Fig. 3). In addition, the overarching stratigraphic framework of northern Mozambique has changed significantly as part of the broader remapping programme and terms such as Lúrio Supergroup are now obsolete. Consequently, we present a completely revised lithostratigraphy for the Monapo Klippe that takes into account the new lithotectonic framework of northern Mozambique (Fig. 3 and Table 1) (e.g. Viola et al., 2008; Bingen et al., 2009; Boyd et al., 2010; Macey et al., 2010).

Although the Monapo Klippe is made up of a significant range of lithologies, nearly all of these can be allocated into three main rock packages (Fig. 3 and Table 1). The first is characterised by strongly deformed high-grade (generally granulite-facies) metamorphic rocks of variable composition hereby defined as the Metachéria Metamorphic Complex. This is the dominant rock unit within the Monapo Klippe. This unit is intruded by two weakly deformed to undeformed suites of igneous rocks, the quartz-bearing Ramiane Suite and the foid-bearing mafic to ultramafic Mazerapane Suite (Fig. 3). In addition to these three main rock units, there are a

number of other lesser rock units whose relationship to the three main rock units remains unclear. The most important of these are the Evate Carbonatite, which is tentatively correlated with the Mazerapane Suite, and the Namialo Pluton, which has characteristics similar to the Ramiane. Finally, the Klippe is everywhere underlain by a mylonitic unit. This unit, hereafter called the Marginal Mylonite, is compositionally variable depending on what rock type is being mylonitised and hence is a tectonic rather than stratigraphic unit. However, because of the significance of this unit for the tectonic evolution of the Monapo Klippe it is here described as a separate unit.

4.1. Metachéria Metamorphic Complex

The Metachéria Metamorphic Complex represents a range of rock types characterised by a high metamorphic grade and a strong penetrative fabric (locally mylonitic). Granulitic gneisses represent the most common rock type of the Metachéria. Two principle types are distinguished, a felsic granulite and a garnet-bearing two-pyroxene mafic granulite. In addition to these granulites, there is a large amount of banded granulite of dominantly intermediate composition intercalated on a variable scale with other rock types of the Metachéria Complex. This rock unit has been termed the undifferentiated granulite. The complex also includes meta-sedimentary gneisses and subsidiary carbonate horizons (Fig. 3 and Table 1). Other rock types, with less well defined protoliths, include quartz-feldspar leucogneiss, feldspathic gneiss, and hornblende gneiss. Some of these units are migmatitic in places, consistent with their granulite-facies grade.

4.1.1. Mafic garnet granulite

The granulitic garnet-bearing mafic rocks occur interbanded/infolded together with the felsic and undifferentiated granulites on an outcrop-scale and as curvilinear horizons up to 200–600 m wide (Fig. 3). They are strongly magnetic and form distinctly mappable units on the geophysical image (Fig. 2d). The rock consists of large garnet poikiloblasts set in a matrix of

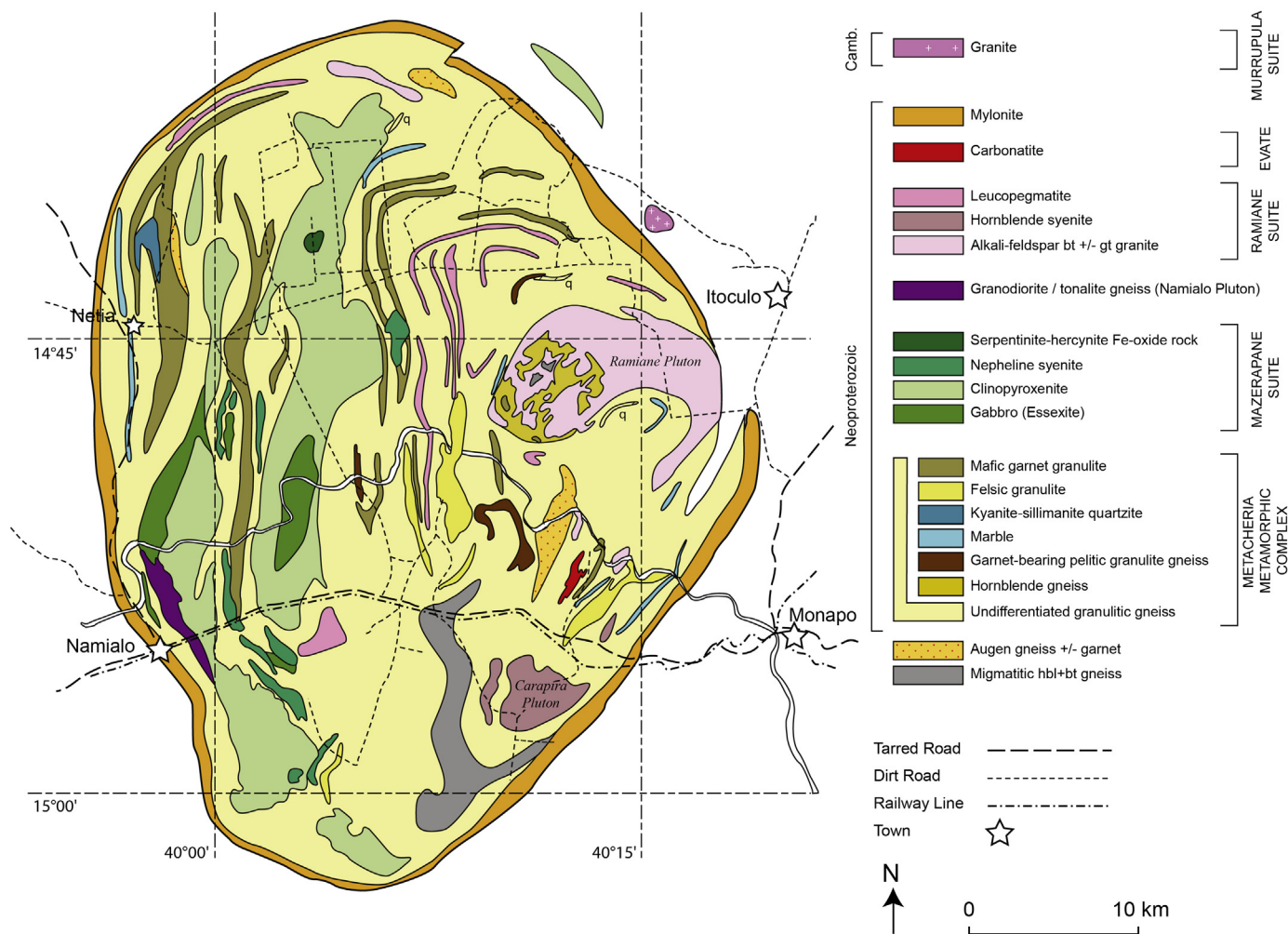


Fig. 3. Geological map of the Monapo Klippe.

clinopyroxene, plagioclase, hornblende (10–15%), orthopyroxene (1–8%), magnetite (1–10%) and quartz (3–5%). These granulites have a weak gneissosity developed in them and do not look migmatitic.

4.1.2. Felsic granulite

Leucocratic quartz-feldspar granulitic leucogneisses are found as bands in the Metachéria Complex in many parts of the Monapo Klippe, but are especially prevalent in the central parts. The leucogneiss is virtually bimimetic, consisting of roughly 25–35% quartz and 65–75% plagioclase. Biotite, muscovite, sphene and magnetite usually occur as accessory phases, but can account for up to 5% of the rock. The rock is strongly deformed as defined by a strong grain flattening fabric in which the quartz occurs as flat tabular-shaped grains (Fig. 4b).

4.1.3. Kyanite-sillimanite quartzite

Kyanite-sillimanite-bearing meta-quartzite with a gneissic fabric crops out in the form of a north-south striking inselberg (Mount Mirué) near the western margin of the klippe. The medium-to coarse-grained meta-quartzite is composed of granoblastic, polygonal quartz (70–95%) together with pokiloblastic sillimanite (10–25%), minor kyanite (1–5%) and rutile (<2%) and finer-grained oxides (2–10%). The meta-quartzite is interspersed with thin foliation parallel sillimanite-rich (~75–100%) layers which consist of coarse- to very coarse-grained radiating acicular blades of sillimanite (Fig. 4c).

4.1.4. Garnet-bearing pelitic granulite gneiss

Pelitic gneisses are not common within the Monapo Klippe and are mostly found in the central parts, interlayered with banded granulites of variable composition. The pelitic gneisses have a banded stromatic migmatitic texture, and contain approximately 10–20% quartz-feldspar leucosomes (Fig. 4d). The palaeosome is comprised of perthite (33%), quartz (15%), plagioclase (2%), biotite (10%), sillimanite (10%) together with considerable amounts of poikiloblastic garnet (30%). Rutile and other opaque oxides occur as accessory minerals. The gneissic fabric is defined by the alignment of biotite, sillimanite and the elongate garnet poikiloblasts.

4.1.5. Marble

Marbles are widely distributed throughout the complex but are not particularly abundant. They occur as flat pavements of very white carbonate often associated with bright orange red soils. These are composed of coarse to very coarse, white to salmon pink calcite grains with or without varying amounts of graphite, olivine, diopside, muscovite, plagioclase, microcline, quartz and minor sulphides.

4.1.6. Hornblende gneiss

Hornblende gneiss is restricted to the country rocks of the Ramíane Pluton that occur SW of Itoculo and shows a weak metre-scale banding due to relatively small variations in the grain size and percentage of mafic minerals. This gneiss is medium-grained and equigranular and is composed of plagioclase (35–60%), hornblende

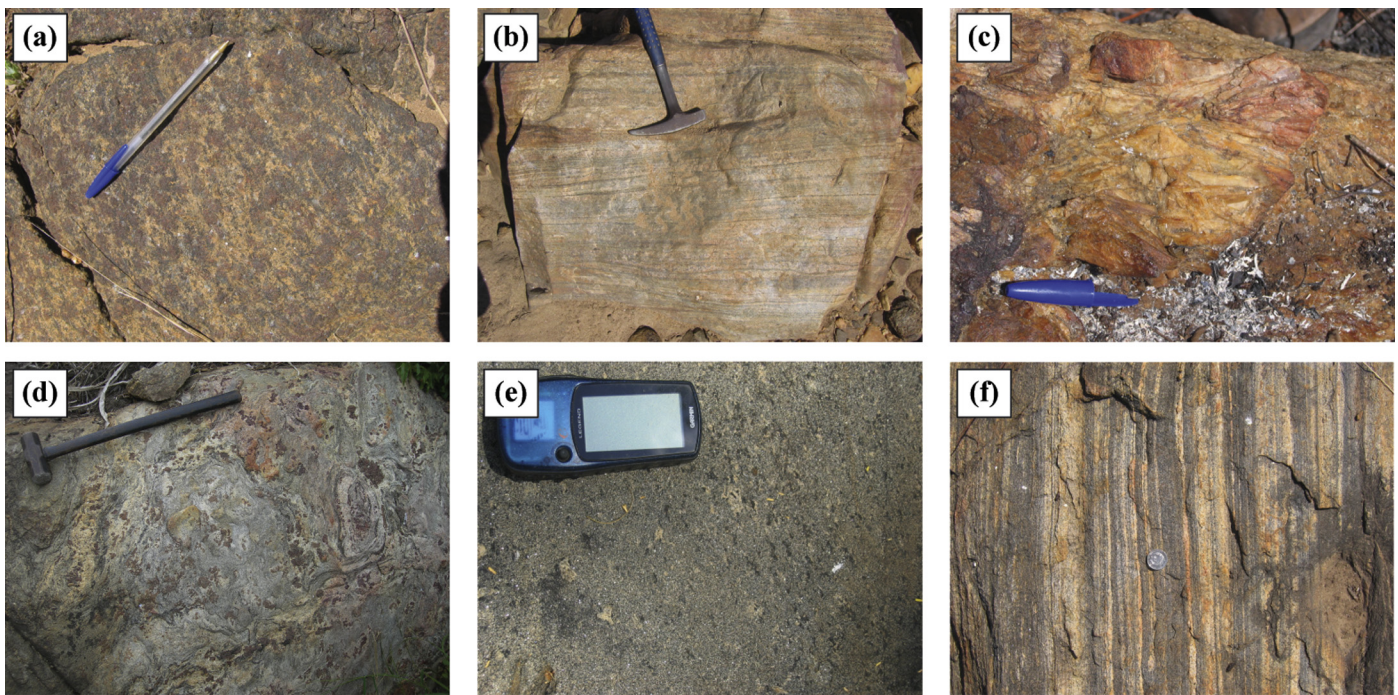


Fig. 4. Field photographs of the Metachéria Metamorphic Complex rocks. (a) Mafic garnet-bearing granulite with weak compositional banding; (b) Strong compositional banding in felsic granulites; (c) Coarse grained sillimanite-kyanite quartzites; (d) Migmatitic garnet + sillimanite granulitic pelites; (e) Spotted hornblende gneiss (contact metamorphism of the Ramiane pluton on the undifferentiated banded gneisses; and (f) Strong compositional banding in the undifferentiated intermediate gneisses.

(~10–20%), biotite (~5–15%), perthitic microcline and orthoclase (5–25%), apatite (1–2%) and opaques (0.5%). Sphene, allanite and calcite occur as accessory minerals. The strong gneissic fabric is defined by the alignment of biotite and amphibole grains and feldspar grain flattening. In the vicinity of the Ramiane Suite granites, the primary gneissic assemblage has been overprinted by porphyroblastic spots of hornblende + biotite (~10–15%) and, less commonly, by spongy blue-green amphibole + opaque + quartz poikiloblasts. These retrograde aggregates probably represent the breakdown of pyroxene under hydrous conditions related to intrusion of the Ramiane Suite granites and leucogranites (Fig. 4e). The gneisses are also cross-cut by minor undeformed coarse-grained hornblende-feldspar veins.

4.1.7. Undifferentiated granulitic gneisses

The undifferentiated granulitic gneisses are dominated by banded granulitic gneisses of variable but generally intermediate composition but also represent a sack unit that includes all of the other units within the Metachéria where they cannot be mapped as individual units. The description given here will thus focus on the banded intermediate gneisses that have not been previously described. These gneisses, in outcrop, are interlayered on a cm to m scale with the meta-sedimentary rocks and the mafic and felsic granulites (Fig. 4f). They are weakly migmatitic (<15%) and have a variable but generally moderate to strong gneissic fabric defined principally by the compositional banding, grain-flattening and the presence of intrafolial folded fabric-parallel leucosomes. Generally they are composed of quartz, plagioclase and K-feldspar in varying proportions although K-feldspar is normally the least abundant phase. Hornblende, biotite and clinopyroxene are present in variable amounts from <5% to a maximum of ±45%.

4.2. Mazerapane Suite

The alkaline ultramafic and mafic rocks of the Mazerapane Suite are restricted to the western half of the Monapo Structure. Four

main undeformed to weakly deformed alkaline ultramafic and mafic intrusive rock units have been identified: (1) clinopyroxenite; (2) nepheline-syenite; (3) foid-bearing gabbros (essexite); and (4) hercynite-serpentinite-Fe-oxide rock.

4.2.1. Clinopyroxenite

The melanocratic black clinopyroxenites are only rarely exposed as small pinnacle-like boulder tors (Fig. 5a) and are more commonly covered by a distinctive dark red-hued clay-rich soil. The rock is usually coarse-grained but grain size varies from 1 to 10 mm and porphyritic varieties also occur. Locally, grain size variations, which are probably a primary magmatic feature, give the rock a weakly banded appearance but the rock is mostly undeformed. Minor amounts of hercynite spinel (<3%), interstitial anorthite ± nepheline (<3%) and trace opaques and calcite are also present. The rocks are locally gabbroic with plagioclase reaching up to modal 15% (Fig. 5a).

4.2.2. Gabbroic rocks

The gabbroic rocks occur as large intrusive bodies in the western central part of the Monapo structure and as sheet-like dykes cross-cutting the Metachéria basement. The rocks consist of plagioclase (50–60%), hornblende (20–25%), clinopyroxene (12–16%) and biotite (1–5%) with minor nepheline (<5%). Apatite, calcite, opaques and retrograde epidote occur in trace amounts. The rock usually has an equigranular granoblastic texture (Fig. 5b). However, some porphyritic gabbros were observed with up to half the plagioclase occurring as large phenocrysts. A weak fabric is defined by a preferred orientation of biotite and the slight alignment of feldspar phenocrysts and hornblende crystals.

4.2.3. Nepheline syenite

The Monapo Klippe contains various small outcrops of undeformed to mylonitic nepheline syenite spatially associated with the clinopyroxenite and gabbro bodies. The syenites display a wide range of grain sizes from medium-grained to pegmatoidal (up to

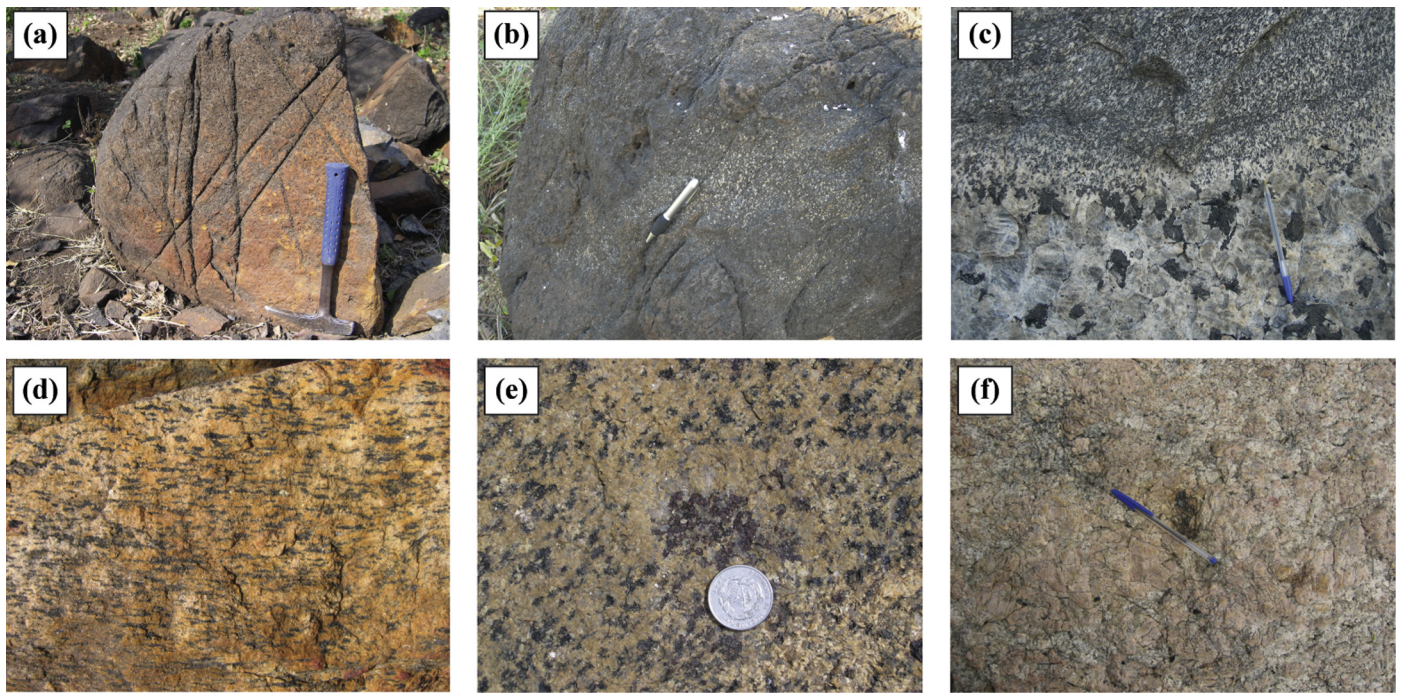


Fig. 5. Field photographs of the Mazerapane and Ramiane Suite rocks. (a) Ultramafic clinopyroxenite of the Mazerapane Suite; (b) Gabbros and clinopyroxenite of the Mazerapane Suite; (c) Nepheline syenite of the Mazerapane Suite showing variation in grainsize and development of pegmatoidal zones. Field relations indicate that the fabric is tectonic and not magmatic. (d) Hornblende syenite (Carapira Pluton) belonging to the Ramiane Suite with weak to moderate fabric development; (e) Alkali-feldspar granite of the Ramiane Suite showing garnet clot and weak fabric development; (f) Leucogranite of the Ramiane Suite.

10–15 cm grainsize – Fig. 5c) and contain (in order of general decreasing abundance) nepheline, orthoclase, microcline, pyroxene heavily altered to biotite, plagioclase, calcite, apatite, muscovite and zircon. The syenite is variably deformed and in places shows a strong mylonitic fabric. Where mylonitised, the pegmatoids consist of large, up to fist-sized, spherical/sigmoidal pyroxene megacrysts (~15%), extensively altered to biotite, sheathed by 5–12 mm thick granoblastic ribbons of nepheline + microcline + plagioclase (~80%) and biotite (~4%). This unit has been grouped together with the Mazerapane Suite pyroxenites because of its geographic association and the presence of nepheline and clinopyroxene in both rock types.

4.2.4. Fe oxide-serpentinite hercynite rock

The ultramafic rocks of the Mazerapane Sub-suite are associated with a rare Fe-oxide-hercynite spinel rock. The undeformed medium- to coarse-grained equigranular rock is comprised of a rusty red/purple and gun metal grey black euhedral oxide mineral (c. 70%; probably hematite) and red-brown Fe-spinel (c. 30%). This rock has been grouped with the Mazerapane Suite because of its ultramafic nature.

4.3. Ramiane Suite

The alkaline Ramiane Suite is made up of variable amounts of alkali-feldspar granite and hornblende syenite that have intruded into the eastern parts of the Monapo Klippe. Hornblende syenite (Fig. 5d) is dominant in the south (Carapira Pluton) while the northern parts (Ramiane Pluton) are dominated by alkali-feldspar granite (Fig. 5e). Numerous leucogranites that occur within the Monapo Klippe (Fig. 5f) have also been grouped with the Ramiane Suite. Previous studies have placed the Evate Carbonatite as part of the Ramiane Suite. However, since there is no obvious link between the carbonatite and the felsic plutonic rocks, in this study the Evate Carbonatite is described as a separate unit.

4.3.1. Alkali-feldspar granite (Ramiane pluton)

The Ramiane pluton is located in the central eastern parts of the Monapo Klippe (Fig. 3). The leucocratic alkali-feldspar granite is medium-grained and equigranular to moderately K-feldspar porphyritic and consists of K-feldspar (60–70%), quartz (15–25%), albitic plagioclase (5–10%) and biotite (10–15%) with minor amphibole (3%). In places garnet occurs as disseminated grains and as part of quartz ± feldspar-garnet patches (Fig. 5e). Magnetite, apatite, zircon and sphene occur as fine-grained accessory minerals. The less common porphyritic varieties contain up to 25% K-feldspar phenocrysts that, when aligned, define a moderate gneissic foliation. The pluton is variably deformed with the core relatively undeformed while the pluton rims display strong fabrics that are almost mylonitic. The fabric follows the edge of the pluton suggesting it developed as the result of the local stress field as the pluton intruded. The Ramiane granite clearly intrudes the rocks of the Metachéria Complex and contains biotite and hornblende gneiss xenoliths, some of which have been stretched parallel to the fabric. The Ramiane Suite plutons are surrounded by a 1–3 km wide zone exhibiting high radiometric signatures which Siegfried (1999) attributed to metasomatic alteration of the country rocks.

4.3.2. Hornblende syenite (Carapira Pluton)

Hornblende syenite is the dominant rock type of the Ramiane Suite in the south eastern parts of the Monapo Klippe where it forms the roughly circular Carapira Pluton (Fig. 3). The medium-grained rock is moderately, but variably, deformed and the alignment of large crystals of black hornblende set in a pale matrix gives the rock a dashed texture (Fig. 5d). The dynamically recrystallised rock is comprised of orthoclase (20%) and plagioclase (10%) and recrystallised porphyroclastic clusters hornblende (10%) and quartz (minor), set in a finer-grained matrix of microcline (~50%), quartz (5%), biotite (2%) and minor opaques. Sphene, zircon, apatite and calcite occur as accessory phases whereas epidote and bundles of muscovite occur as retrograde minerals. The hornblende

syenite contains xenoliths of biotite gneiss and is locally cross-cut by discrete shear zones.

4.3.3. Leucopegmatites

Undeformed bodies and dykes of leucocratic pale-pink to cream coloured pegmatite occur throughout the Monapo Klippe but are most prevalent in the central parts. Field observations indicate the pegmatites consist of K-feldspar (~64%) and quartz (~33%) together with biotite (~3%) and small amounts of euhedral magnetite. The quartz and feldspar grain-size varies on an outcrop-scale from coarse-grained (10 mm) to very coarse-grained (30–100 mm) (Fig. 5f). The undeformed pegmatites cross-cut the plutonic rocks of the Ramiane Suite, but it remains unclear if they are late stage fractionates of these intrusive rocks, or if they represent younger rocks (i.e. Murrupula Suite).

4.4. Marginal mylonite

The boundary of the Monapo Klippe with the underlying Nampula Block gneisses is delineated by a continuous zone of mylonite and blastomylonite (Fig. 3). The sheared rocks are only locally exposed, but are easily traced out on both the satellite and geophysical images (Fig. 2). The dominant composition is a quartzo-feldspathic mylonite that has undergone extensive recrystallisation. The mylonite is typically only a few metres thick, with a pervasive planar shear fabric (Fig. 6a). The quartz-feldspar matrix is uniformly fine grained and equigranular. Original shear textures are observed on hand sample to outcrop scales but the subhedral interlocking grain microstructure is consistent with total static recrystallization overprinting shear microtextures. Grains with extended tails are highly symmetrical (Fig. 6a), suggesting a high degree of shear strain and flattening. Asymmetrical grain tails and clasts are very rare but suggest top to the east motion. However, since the Monapo Klippe appears to have been folded during subsequent emplacement (see below), this cannot necessarily be

interpreted to represent the transport direction at the time of formation of the mylonite.

4.5. Other rock types

4.5.1. Quartz bodies

Syn-tectonic, foliation parallel quartz veins are found throughout the Metachéria Complex ranging in size from small outcrop veins to large km-scale lenticular bodies. The veins are comprised of equigranular coarse-grained dynamically recrystallised quartz with minor, completely weathered, K-feldspar. Minor subsequent deformation is indicated by alignment of weathered feldspar.

4.5.2. Evate carbonatite

The Evate carbonatite is situated in the south eastern parts of the Monapo Klippe, 10 km NW of Monapo village (Monapo Map). The poorly exposed body can be traced for approximately 3 km and is up to 700 m wide, striking SW and dipping NW conformable to the host gneisses of the Metachéria Complex. The calcitic carbonatite is medium- to very coarse-grained with variable amounts of apatite, magnetite, pyrrhotite and diopside (Fig. 6b). Numerous other minerals are associated with the carbonatite including but not limited to forsterite, phlogopite, graphite, and beryl. A large K-fenite aureole is developed around the margins of the carbonatite which supports an intrusive origin.

4.5.3. Granodiorite-tonalite (Namialo Pluton)

A 500 m-wide foliation-parallel body of equigranular tonalitic-granodioritic gneiss is exposed in a large road aggregate quarry approximately 2 km northeast of Namialo. The intrusive body can be traced on the geophysical images as a distinct unit stretching over 12 km north-south. The sheared leucocratic grey rock has a strong sub-mylonitic fabric in one plane (Fig. 6c) with the dynamically recrystallised plagioclase porphyroclasts being replaced by

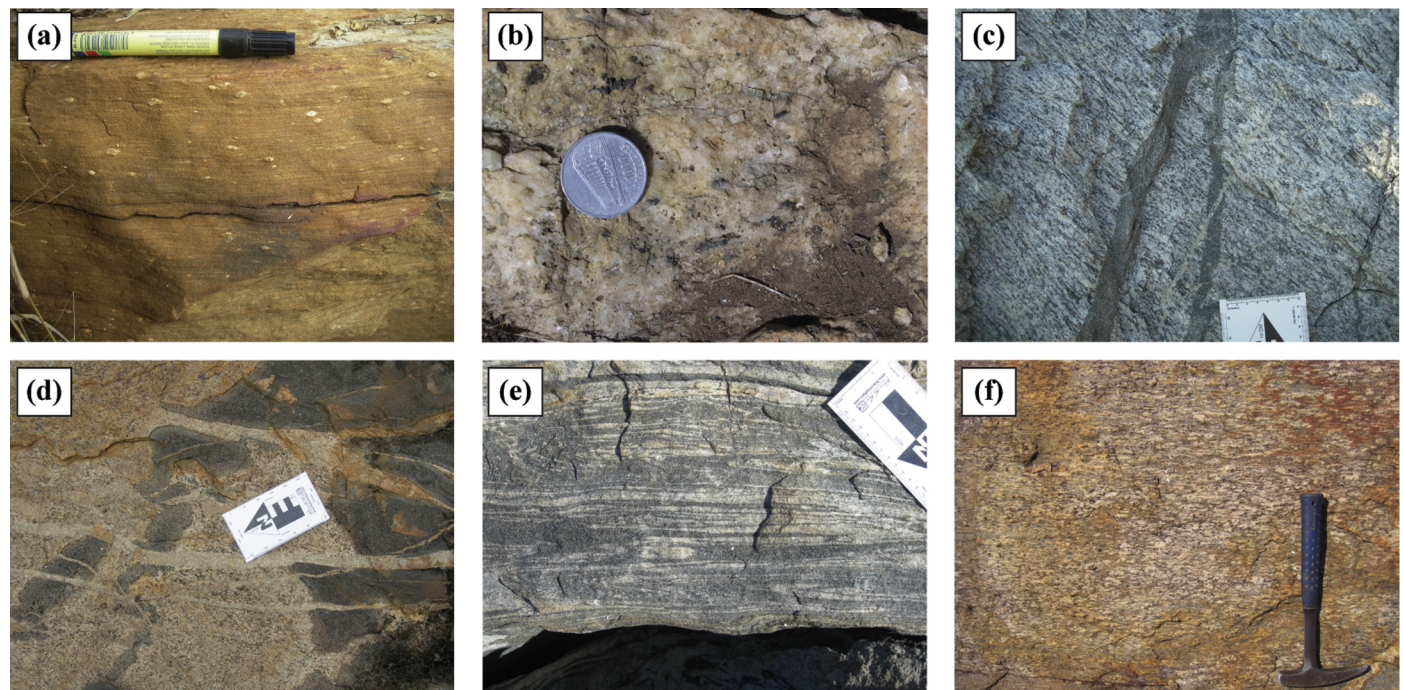


Fig. 6. Other rock units of the Monapo Klippe. (a) Quartzo-feldspathic marginal mylonite showing symmetrical quartz clasts; (b) Evate carbonatite with large pale green apatite crystals; (c) Granodiorite-tonalite from the Namialo Pluton showing moderate fabric development and cross cutting mafic dyke; (d) Granodiorite-tonalite from outside the Namialo Quarry showing much weaker fabric development along with disaggregated mafic material and cross-cut by felsic dykes; (e) Strongly deformed migmatitic hornblende-biotite gneiss; (f) Streaky augen garnet-bearing gneiss.

granular aggregates of quartz and plagioclase. The main mafic mineral is biotite.

4.5.4. Migmatitic hornblende-biotite gneiss

A ~2–5 km wide band of migmatitic grey hornblende-biotite gneiss crops out in the southern central part of the Monapo Klippe. The gneiss differs from the surrounding Metachéria gneisses in the degree of migmatisation and general appearance and has a similar degree of migmatisation to the surrounding Nampula gneisses. In addition, the rocks are variably mylonitised (Fig. 6e) but are usually strongly retrogressed in thin-section with hornblende being altered to biotite. Medium-sized irregularly shaped magnetite grains are strongly associated with the hornblende. The matrix is dominantly plagioclase (70–85%) with sericitic alteration. The overall texture is bimodal with large quartz grains sitting in a finer granoblastic matrix of plagioclase + quartz + hornblende + biotite + magnetite.

4.5.5. Streaky garnet-bearing augen gneiss

This leucocratic cream-coloured streaky augen gneiss consists of completely recrystallised feldspar augen set in an equigranular matrix of quartz and feldspar, streaks of biotite and disseminated ~1 mm porphyroblasts of garnet with minor clinopyroxene partially retrogressed to hornblende (Fig. 6f). The strong penetrative gneissic fabric is cross cut by a discrete crenulation cleavage. Large irregularly shaped but elongate magnetite is associated with the hornblende and sits aligned within the gneissic fabric.

5. Geochemistry

A total of 34 representative samples of the major lithodemic units of the Monapo Klippe were selected for major and trace element geochemical analysis. Samples were selected from the least altered and weathered outcrops. The samples were analysed by ICP-AES and ICP-MS by N. Walsh at the ICP Laboratory at Royal Holloway, University of London. Analytical techniques are described in Appendix 1 and the geochemical data are presented in Supplementary Table S1. Although major element correlations are relatively consistent across most of the major rock units, spider diagrams show variable amounts of open system behaviour in the mobile elements (alkalis, Ba, Rb) with the exception of the Ramiane Suite rocks which show coherent geochemical trends. The Mazerapane Suite also shows considerable open system behaviour in the mobile elements in comparison to other lithodemic units including the high-grade granulitic units. Despite these problems, the geochemical character of all the units can still provide useful information towards understanding the origin of the rock types and their tectonic assembly.

Supplementary material related to this article found, in the online version, at <http://dx.doi.org/10.1016/j.plantsci.2004.08.011>.

5.1. Metachéria Metamorphic Complex

The rocks of the Metachéria Metamorphic Complex do not preserve any unequivocal evidence for primary sedimentary or volcanic textures and inferences around the origin of these rock types are based on mineralogy and geochemical composition. Seven samples of the garnet two-pyroxene mafic granulite, four of the undifferentiated mafic + intermediate granulites and four samples of the felsic granulites were analysed and the results shown in Figs. 7–9. The felsic granulites are clearly compositionally distinct from the mafic and intermediate gneisses. The felsic granulites plot as meta-rhyolites and meta-dacites on the total alkali versus silica diagram (Fig. 7a) and are characterised by moderately high to high SiO₂ (67.4–75.9 wt% SiO₂), very low Fe_{Total} (<6.5 wt%) and CaO (<5.5 wt%), negligible MgO (max 1.8 wt%) and variable K₂O contents. In contrast, the mafic granulites and mafic + intermediate

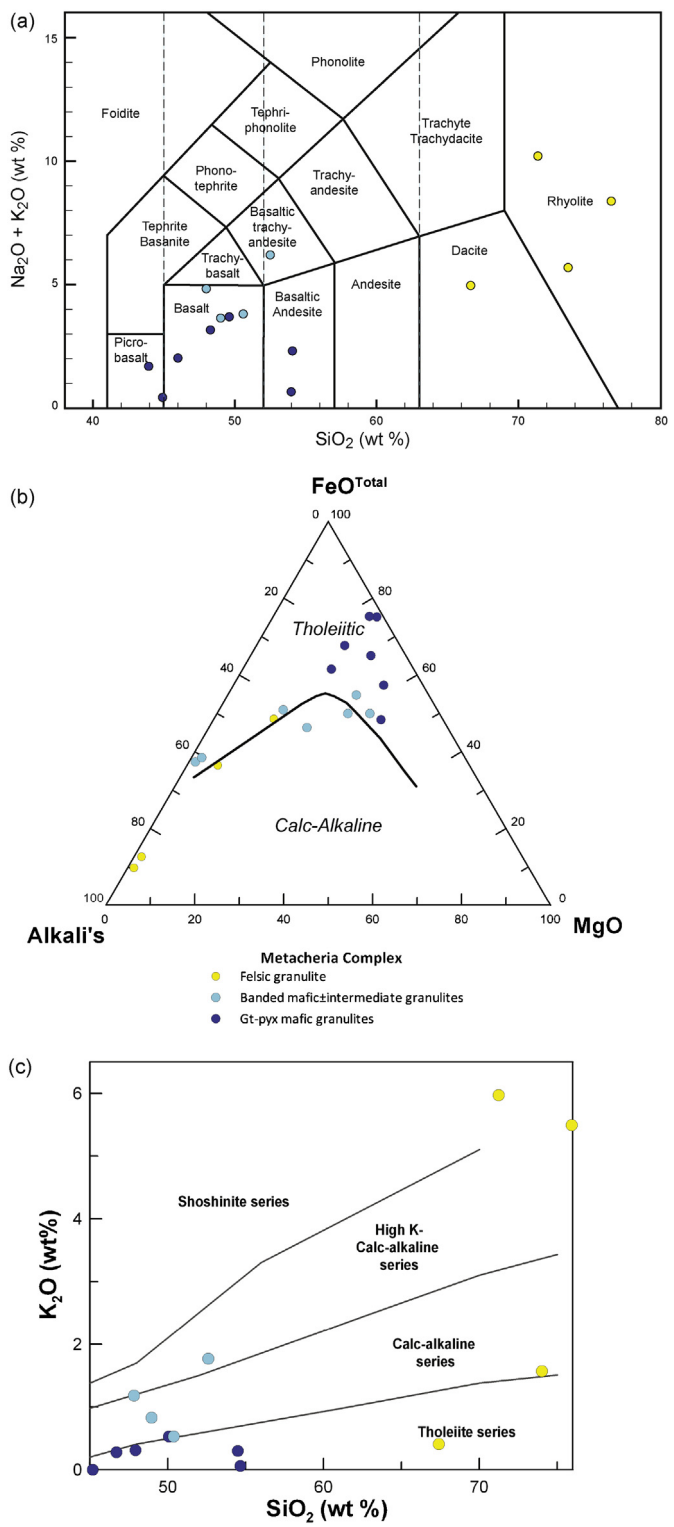


Fig. 7. Geochemical diagrams of the Metachéria Metamorphic Complex. (a) Silica versus alkalis (TAS) diagram, with fields after Cox et al. (1979); (b) AFM after Irvine and Barager (1971); (c) silica versus K₂O magma discrimination after Peccerillo and Taylor (1976).

granulites plot as basalts to basaltic-andesites (Fig. 7a). Some samples are more mafic plotting as picro-basalts while others have elevated alkali contents and plot as trachy-basalts and trachy-andesites. Fe_{Total} is considerably higher than the felsic granulites (min 9 wt%), along with MgO (min 4.3 wt%) and CaO (min 7.7 wt%) although the content of these elements can be variable. Within the

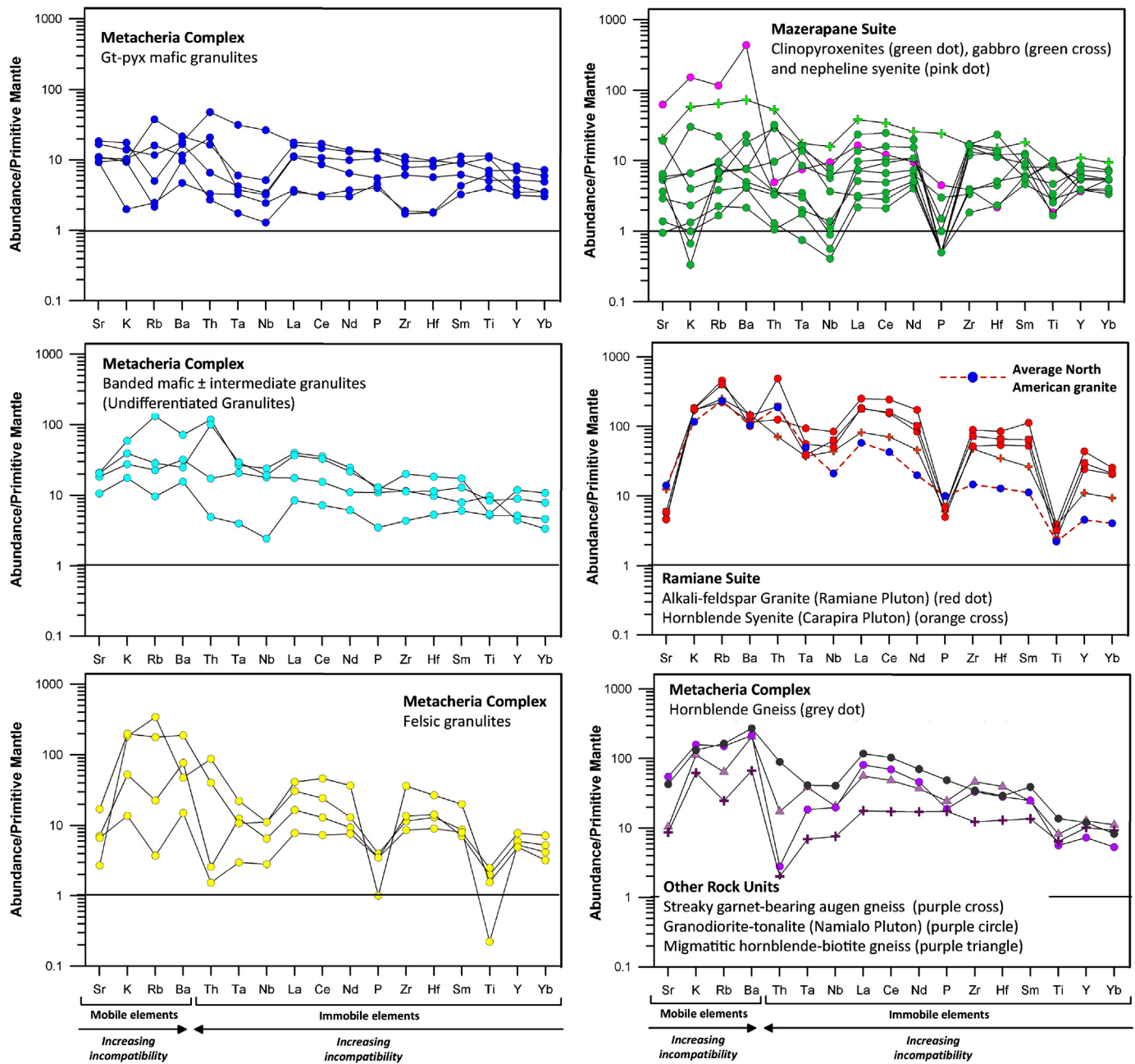


Fig. 8. Primitive mantle normalised trace element diagrams for the main lithodemic units of the Monapo Klippe. Normalisation values after Sun and McDonough (1989). (a) Metachéria mafic granulites; (b) Metachéria undifferentiated mafic and intermediate granulites; (c) Metachéria felsic granulites; (d) Mazerpane Suite intrusives; (e) Ramiane Suite intrusives; (f) inferred basement gneisses and other orthogneisses within the Monapo Klippe.

mafic granulites K_2O is negligible but in the mafic + intermediate granulites it is variable although in lower concentrations than the felsic gneisses.

The garnet two-pyroxene mafic granulites have tholeiitic trends on an AFM diagram and the K_2O vs. SiO_2 diagram whereas the undifferentiated mafic + intermediate granulites trend towards more calc-alkaline compositions (Fig. 7b and c). The felsic granulites have variable compositions between shonshonitic and tholeiitic (Fig. 7c). Chondrite normalised REE patterns for the garnet two-pyroxene mafic granulites (Fig. 9a) indicate very flat REE concentrations ($La_N/Yb_N \approx 2.0$) around $10\times$ chondrite with no clear Eu anomaly ($Eu/Eu^* = 1.07 \pm 0.15$) and hence have very similar compositions to E-MORB. In contrast, both the intermediate and felsic granulites are more LREE enriched ($La_N/Yb_N \approx 3.7$ intermediate

granulites and ≈ 5.7 felsic granulites) and show weak Eu anomalies ($Eu/Eu^* = 0.85$) in the intermediate granulites and moderate Eu anomalies ($Eu/Eu^* = 0.67$) in the felsic granulites (Fig. 9b and c). Primitive mantle normalised trace element diagrams show significant scatter in the mobile elements but most samples show some degree of negative Ta–Nb anomaly normally indicative of arc-derived magmas or the remelting of rocks formed in arc settings (Fig. 8). The felsic granulites (Fig. 8c) differ from the mafic and intermediate granulites (Fig. 8a and b) in that they also show pronounced negative P and Ti anomalies and higher concentrations of Rb, Ba, K and Th similar to the Ramiane Suite intrusives and the Rapale and Mocuba Gneisses and Culicui Suite granites in the Nampula Block (Macey et al., 2010). Tectonic discrimination diagrams indicate that the mafic and intermediate granulites

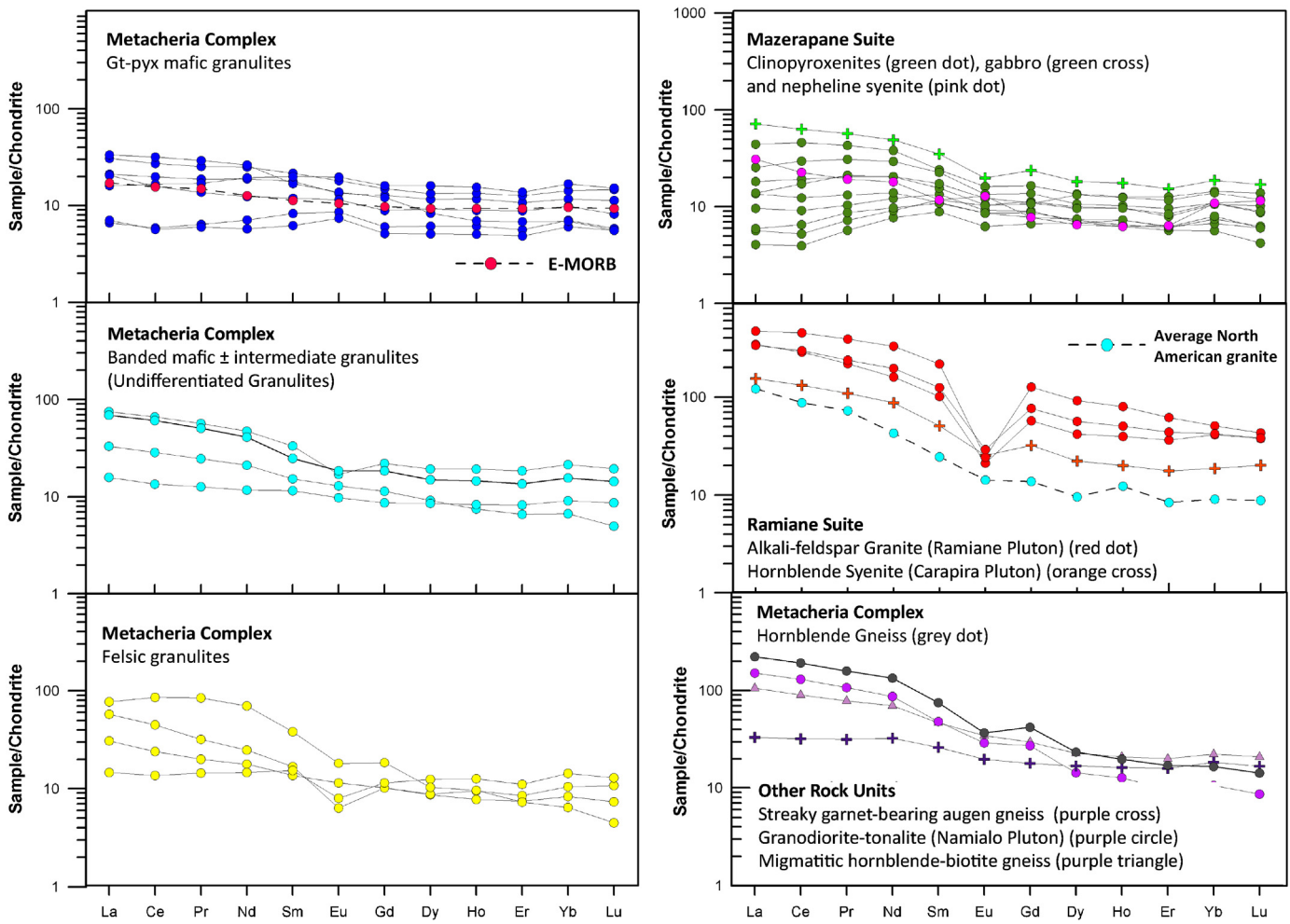


Fig. 9. Chondrite normalised REE diagrams for the main lithodemic units of the Monapo Klippe. Normalisation values after Sun and McDonough (1989). (a) Metachéria mafic granulites; (b) Metachéria undifferentiated mafic and intermediate granulites; (c) Metachéria felsic granulites; (d) Mazerpane Suite intrusives; (e) Ramiane Suite intrusives; (f) inferred basement gneisses and other orthogneisses within the Monapo Klippe.

have MORB or Island-arc-tholeiite type affinities (Pearce and Norry, 1979; Meschede, 1986).

5.2. Mazerpane Suite

Nine samples of the clinopyroxenite, one sample of the gabbro and one of the nepheline syenite were analysed and the results shown in Figs. 8–10. The clinopyroxenites have clearly very mafic compositions with MgO contents ranging from 10.2 to 20.0% (mean $13.3 \pm 3.2\%$) with Mg numbers generally primitive in character (0.57–0.70) (Fig. 10a and Table S1). These rocks are silica undersaturated and have variable amounts of nepheline present. The nepheline syenite contains approximately 10–15% nepheline when undeformed with over 13 wt% Na₂O + K₂O (Table S1). Primitive mantle normalised trace element patterns (Fig. 8d) are erratic for the Mazerpane suite clinopyroxenites and indicate partial remobilisation of elements. A clear negative P anomaly can be seen, but only some of the rocks have a Ti anomaly and it is difficult to see a consistent Ta–Nb anomaly. The Ta–Nb anomaly is not present in the nepheline syenite. Chondrite normalised REE diagrams (Fig. 9d) indicate fairly flat patterns around 10× chondrite with total REE concentrations less than 200 ppm and typically less than 100 ppm. The samples show variable LREE enrichment with three samples having values less than 1 (i.e. actually HREE enrichment), while the other six samples had La_N/Yb_N values between 1.3 and 2.4. The Mazerpane Suite rocks define a tholeiitic trend on the AFM

diagram (Fig. 10b), but the one sample of gabbro is transitional to calc-alkaline in composition while the nepheline syenite is shoshonitic in composition.

5.3. Ramiane Suite

Three samples of the Ramiane Pluton granite and one of the Carapira Pluton hornblende syenite were analysed and clear differences between the two rock types were recorded (Table S1 and Figs. 8–10). The granite samples have 68–70 wt% SiO₂, 13–14 wt% Al₂O₃, 2–2.5 wt% CaO, 2.7–2.8 wt% Na₂O and 5.0–5.5 wt % K₂O (Table S1). In comparison the single sample of the hornblende syenite had lower wt% SiO₂ (~63 wt%), higher Al₂O₃ (~17.5 wt%), similar CaO and K₂O contents, but higher Na₂O contents (~4.8 wt%). All samples have high Ba (>700 ppm), Zr (>500 ppm), are enriched in the LREE (La/Yb_N > 8) with pronounced negative Eu anomalies (Eu/Eu* = 0.3–0.1) although the Eu anomaly in the Carapira syenite is not as pronounced with a value of 0.6 (Table S1). Normatively the granites are monzogranites while the hornblende syenite plots as a quartz monzonite. This discrepancy between the modal mineralogy and the normative mineralogy is likely related to the perthitic nature of the K-feldspar. The alumina saturation index range for all samples is in excess of 1.3 indicating that the granites are peraluminous. On the Ga/Al vs Ce + Zr + Nb + Y and Zr vs Ga/Al classification diagrams (Fig. 10c) of Whalen et al. (1987), all the samples plot as A-Type granites. The Ramiane suite rocks classify as type A2 (Fig. 10e)

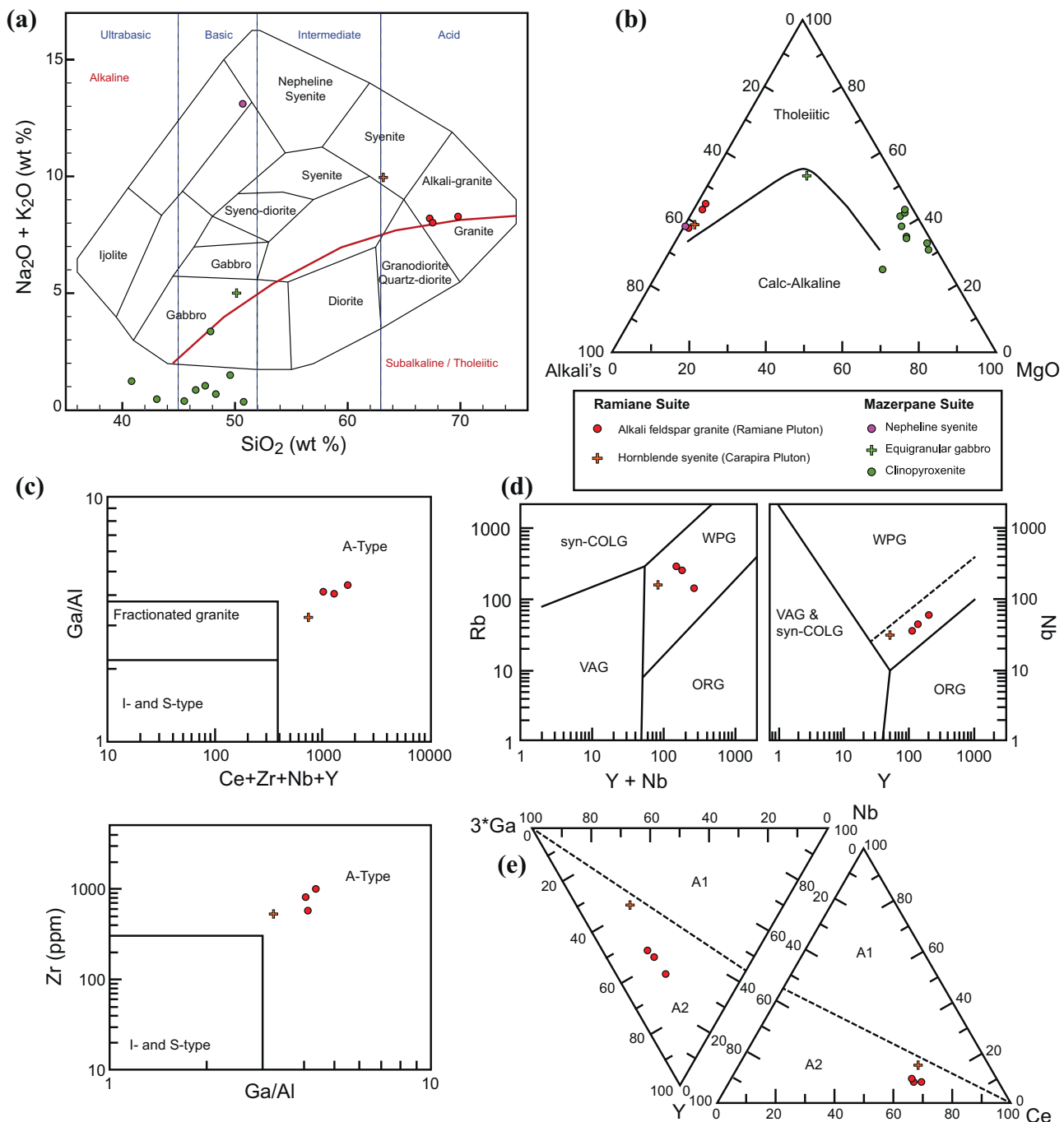


Fig. 10. Geochemical diagrams of the Mazerpane and Ramiane suite rocks. (a) Silica versus alkalis (TAS) diagram for plutonic rocks, with fields after Cox et al. (1979); (b) AFM after Irvine and Barager (1971); (c) Zr versus Ga/Al and Ga/Al versus Zr + Ce + Nb + Y plots after Eby (1992); (d) Rb versus Y + Nb and Nb versus Y plots, after Pearce et al. (1984); (e) Y-Nb-Ce and Nb-Y-3*Ga plots after Edy (1992). Granite acronyms: syn-COLG – syn collision; VAG – volcanic arc; WPG – within plate; ORG – ocean ridge.

on the Nb–Ce–Y and Nb–Y–3*Ga plots of Eby (1992) indicating that they are characteristic of A-type granitic melts derived from continental crust. In this respect they are similar to the c. 1075 Ma Culicui Suite granites and the 535–495 Ma Murrupula Suite granites in the Nampula Block, both of which were interpreted to have formed in a late tectonic extensional setting (Macey et al., 2007, 2010).

5.4. Other rock types

Four other samples from the Monapo Klippe were analysed for their geochemical composition (Table S1, Figs. 8f and 9f). These are one each of the hornblende orthogneiss surrounding

the Ramiane Pluton, which is considered part of the Metachéria Metamorphic Complex, the sheared augen gneiss, the migmatitic hornblende + biotite gneiss and the granodiorite/tonalite of the Namialo Pluton. The sheared augen gneiss and the migmatitic hornblende + biotite gneiss are considered part of the basement rocks and have been mapped as windows of Nampula Gneisses that outcrop through the base of the Monapo Klippe. However, their geochemical character is sufficiently different to any of the Nampula Gneisses that it is difficult to support this contention. On the trace element spider diagram, the Nampula gneisses all have prominent negative P and Ti anomalies as well as either a strong negative Ba anomaly, a strong Nb-Ta anomaly or both, with

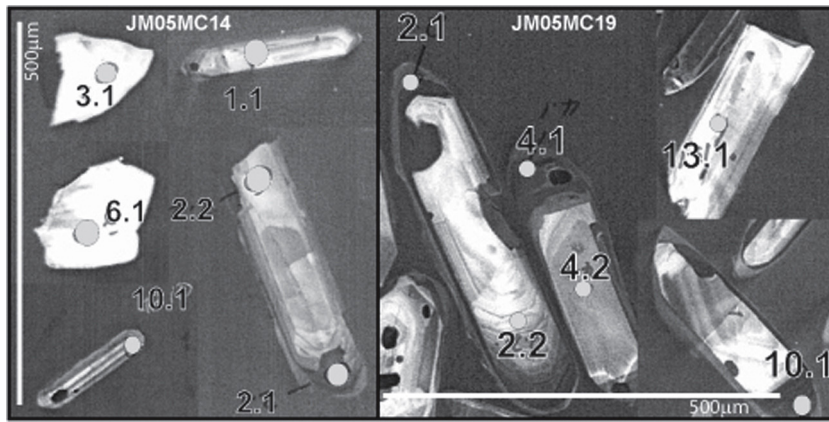


Fig. 11. Cathodoluminescence (CL) images of representative zircons with analysed spots indicated and referenced to analysis points in Tables 2 and 3.

the exception of the Molóquè Group mafic gneisses which have relatively flat trace element patterns. On REE diagrams, the Nam-pula Gneisses have moderate to steep REE patterns, with LREE enrichment with or without a pronounced negative Eu anomaly again with the exception of the Molóquè Group mafic gneisses which have again relatively flat REE patterns. In contrast, while the streaky augen gneiss and the migmatitic hornblende + biotite gneiss have REE patterns similar to the Mamala Gneiss or Culicui Suite (Fig. 9f), the trace element spider diagrams are dissimilar with only very weak negative P and Ti anomalies present, a prominent Th anomaly and as a result no clear Nb-Ta anomaly (Fig. 8f). The hornblende gneiss surrounding the Ramiane Pluton is very similar to the Metachéria intermediate gneisses which is to be expected. The Namialo Pluton rocks have similar REE patterns to the Metachéria intermediate granulites and some similarities to the trace element spider diagrams of the same rocks particularly in that they also have a negative Th anomaly. However, the differences in the physical appearance and mineralogy of this unit make it a distinct unit although it is unclear what its relationship to other rock units within the Monapo is.

6. Geochronology

Three ages have been previously reported from the Monapo Complex. Siegfried (1999) reported a zircon age of 590 Ma from the Evate Carbonatite and a Mazerapane pyroxenite but no further information as to the locality or analytical method was specified. Jamal (2005) dated a leuco-gneiss from the Namialo Pluton using the SHRIMP U-Pb technique on zircon and obtained a pooled age of 635 ± 3.1 Ma based on 11 spot analyses. Although the zircons exhibited core and overgrowth structures, these individual zones yielded indistinguishable dates of 632.0 ± 14 Ma and 638.2 ± 4.4 Ma ($\text{MSWD} = 0.52$), respectively. On this basis, the magmatic and metamorphic events were interpreted to be nearly contemporaneous with the intrusion of the Namialo Pluton (Jamal, 2005). An undeformed aplite vein from the Namialo Pluton was also dated and yielded a SHRIMP U/Pb age of 559 ± 9 Ma (Jamal, 2005). This age is inferred to be the minimum age for the latest deformation of the klippe.

In view of the uncertainty of the ages of these rocks, two samples were selected for SHRIMP U-Pb zircon dating as part of this study. They were a two-pyroxene mafic garnet granulite (JM05MC14) from the Metachéria Metamorphic Complex ($14^{\circ}44.381' S$; $40^{\circ}02.652' E$) and a granite (JM05MC19) of the Ramiane Suite ($14^{\circ}48.237' S$; $40^{\circ}16.915' E$). The samples were analysed at the Australian National University in Canberra, Australia using a SHRIMP II instrument. Analytical techniques are given in

Appendix 1 and the data is presented in Tables 2 and 3. Cathodoluminescence (CL) images of typical zircons analysed from selected samples are given in Fig. 11. Dates are specified to 2σ standard deviations, although data ellipses in Fig. 12 are given as 1σ standard deviation.

6.1. Ramiane Suite (alkali feldspar granite JM05MC19)

Sample JM05MC19 is a biotite-bearing alkali feldspar granite with minor almandine-rich garnet present. One population of

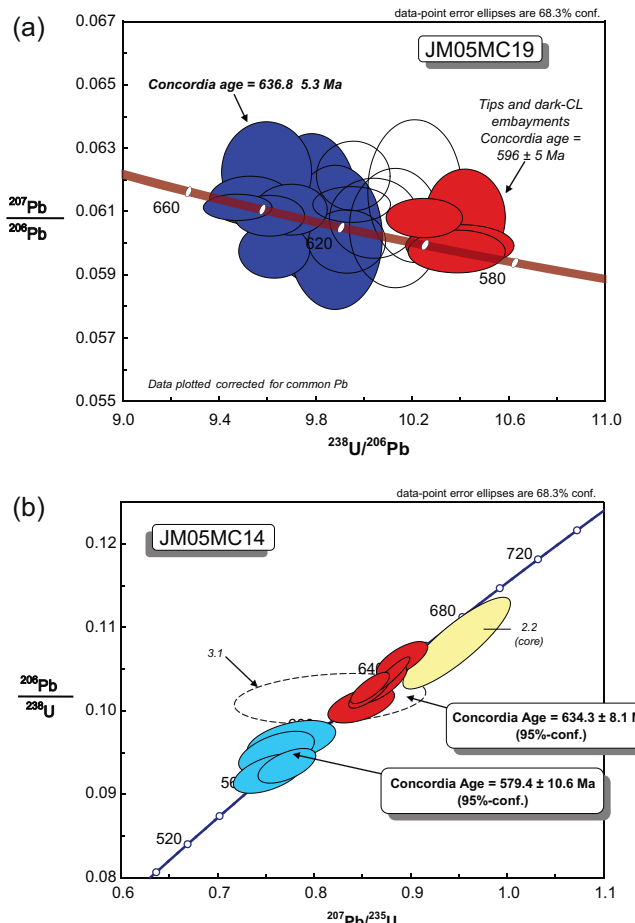


Fig. 12. Concordia plots for (a) Metachéria garnet two-pyroxene mafic granulite JM05MC14 and (b) alkali-feldspar granite of the Ramiane Suite JM05MC19.

Table 2
SHRIMP U–Pb data from zircons from sample JM05MC19.

Grain, spot	% $^{206}\text{Pb}_c$	ppm U	ppm Th	$^{232}\text{Th}/^{238}\text{U}$	ppm $^{206}\text{Pb}^*$	(1) $^{206}\text{Pb}/^{238}\text{U}$ Age	(1) $^{207}\text{Pb}/^{206}\text{Pb}$ Age	% Discordant	Total $^{238}\text{U}/^{206}\text{Pb}$	±%		
1.1	0.73	931	152	0.17	80.9	617	± 5.9	677	± 25	9	9.883	10
2.1	0.00	656	123	0.19	54.2	592.8	± 7.2	593	± 16	0	10.38	1.3
2.2	0.27	91	25	0.28	8.05	627.3	± 7.7	642	± 54	2	9.76	1.3
4.1	0.00	582	104	0.18	48.8	600.2	± 5.8	631	± 15	5	10.25	1
4.2	0.00	110	43	0.40	9.34	607	± 7.1	620	± 44	2	10.13	1.2
5.1	0.41	850	171	0.21	76.1	636.9	± 6.1	594	± 21	-7	9.59	1
6.1	0.02	1507	194	0.13	136	643.1	± 7.2	650	± 18	1	9.53	1.2
6.2	0.00	93	27	0.30	8.28	638.8	± 7.8	681	± 36	6	9.6	1.3
7.1	0.09	339	96	0.29	28	590.9	± 6	631	± 36	6	10.41	1.1
8.1	0.02	1370	201	0.15	124	646.6	± 6.1	642.8	± 9.7	-1	9.476	0.99
9.1	0.12	791	137	0.18	70.8	638.2	± 6.1	633	± 15	-1	9.598	10
10.1	0.05	772	123	0.17	66.8	618.5	± 6.3	604	± 24	-2	9.92	1.1
11.1	0.11	1378	84	0.06	119	617.4	± 6.2	646	± 13	4	9.94	1.1
12.1	0.00	1214	81	0.07	100	592.1	± 8	599	± 16	1	10.39	1.4
13.1	0.28	107	40	0.39	9.29	621.5	± 7.7	609	± 54	-2	9.85	1.3
14.1	0.00	148	46	0.32	12.7	612.1	± 7	630	± 29	3	10.04	1.2
14.2	0.07	653	145	0.23	57.9	632.6	± 6.1	640	± 19	1	9.692	1
15.1	0.19	125	39	0.33	10.5	602.4	± 7.2	660	± 52	9	10.19	1.2
Grain, spot	Total $^{207}\text{Pb}/^{206}\text{Pb}$	±%	(1) $^{238}\text{U}/^{206}\text{Pb}^*$	±%	(1) $^{207}\text{Pb}^*/^{206}\text{Pb}^*$	±%	(1) $^{207}\text{Pb}^*/^{235}\text{U}$	±%	(1) $^{206}\text{Pb}^*/^{238}\text{U}$	±%	Err. corr.	
1.1	0.06808	0.5	9.956	1	0.06208	1.2	0.86	1.5	0.1004	1	.654	
2.1	0.0597	0.74	10.38	1.3	0.0597	0.74	0.793	1.5	0.0963	1.3	.864	
2.2	0.0633	1.7	9.78	1.3	0.0611	2.5	0.861	2.8	0.1022	1.3	.452	
4.1	0.06076	0.68	10.25	1	0.06076	0.68	0.8174	1.2	0.09758	1	.830	
4.2	0.0604	2.1	10.13	1.2	0.0604	2.1	0.823	2.4	0.0987	1.2	.512	
5.1	0.06309	0.54	9.63	1	0.05973	0.96	0.855	1.4	0.1038	1	.722	
6.1	0.06144	0.82	9.53	1.2	0.0613	0.83	0.887	1.4	0.1049	1.2	.819	
6.2	0.0622	1.7	9.6	1.3	0.0622	1.7	0.894	2.1	0.1042	1.3	.604	
7.1	0.06152	1.5	10.42	1.1	0.0608	1.7	0.804	2	0.096	1.1	.537	
8.1	0.06125	0.44	9.478	0.99	0.0611	0.45	0.8888	1.1	0.1055	0.99	.910	
9.1	0.06181	0.56	9.609	10	0.06083	0.7	0.873	1.2	0.1041	10	.817	
10.1	0.06045	1.1	9.93	1.1	0.06002	1.1	0.833	1.5	0.1007	1.1	.693	
11.1	0.06208	0.49	9.95	1.1	0.06119	0.61	0.848	1.2	0.1005	1.1	.866	
12.1	0.05987	0.73	10.39	1.4	0.05987	0.73	0.794	1.6	0.0962	1.4	.888	
13.1	0.0624	1.9	9.88	1.3	0.0602	2.5	0.839	2.8	0.1012	1.3	.463	
14.1	0.06075	1.4	10.04	1.2	0.06075	1.4	0.834	1.8	0.0996	1.2	.663	
14.2	0.06162	0.66	9.699	1	0.06103	0.86	0.868	1.3	0.1031	1	.760	
15.1	0.0632	1.9	10.21	1.3	0.0616	2.4	0.832	2.7	0.0979	1.3	.461	

Errors are 1 – sigma; Pb_c and Pb^* indicate the common and radiogenic portions, respectively.

Error in standard calibration was 0.31% (not included in above errors but required when comparing data from different mounts).

(1) Common Pb corrected using measured ^{204}Pb .

Table 3
SHRIMP U–Pb data from zircons from sample JM05MC14.

Grain, spot	% $^{206}\text{Pb}_c$	ppm U	ppm Th	$^{232}\text{Th}/^{238}\text{U}$	ppm $^{206}\text{Pb}^*$	(1) $^{206}\text{Pb}/^{238}\text{U}$ age	(1) $^{207}\text{Pb}/^{206}\text{Pb}$ age	% Discordant	Total $^{238}\text{U}/^{206}\text{Pb}$	±%		
1.1	0.00	480	106	0.23	42.5	632.4	±8.4	650	±24	3	9.7	1.4
2.1	0.00	1713	112	0.07	153	639	±8.1	645	±13	1	9.6	1.3
2.2	0.00	149	43	0.30	13.8	661	±21	727	±41	9	9.26	3.4
3.1	0.90	64	11	0.18	5.62	622	±12	543	±170	-15	9.78	1.9
4.1	0.00	82	9	0.11	6.66	584.2	±9.8	534	±65	-9	10.54	1.8
5.1	0.30	90	11	0.12	7.5	592.1	±9.7	546	±76	-8	10.36	1.7
6.1	0.00	83	14	0.17	6.55	569.3	±9.2	569	±59	0	10.83	1.7
7.1	0.00	157	38	0.25	12.6	574.8	±8.2	601	±45	4	10.72	1.5
8.1	0.28	226	86	0.39	19.5	617.8	±8.3	644	±49	4	9.91	1.4
9.1	0.07	1401	241	0.18	124	629.8	±7.3	623	±21	-1	9.74	1.2
10.1	0.00	291	121	0.43	26.5	649.6	±8.3	635	±30	-2	9.43	1.3
11.1	0.00	490	130	0.27	43	627.3	±7.7	631	±23	1	9.79	1.3
Grain, spot	Total $^{207}\text{Pb}/^{206}\text{Pb}$	±%	(1) $^{238}\text{U}/^{206}\text{Pb}^*$	±%	(1) $^{207}\text{Pb}^*/^{206}\text{Pb}^*$	±%	(1) $^{207}\text{Pb}^*/^{235}\text{U}$	±%	(1) $^{206}\text{Pb}^*/^{238}\text{U}$	±%	Err. corr.	
1.1	0.06131	1.1	9.7	1.4	0.06131	1.1	0.871	1.8	0.1031	1.4	.780	
2.1	0.06117	0.61	9.6	1.3	0.06117	0.61	0.879	1.5	0.1042	1.3	.911	
2.2	0.0636	2	9.26	3.4	0.0636	2	0.947	3.9	0.108	3.4	.864	
3.1	0.0657	3.1	9.87	2	0.0584	7.8	0.816	8	0.1014	2	.245	
4.1	0.0581	3	10.54	1.8	0.0581	3	0.76	3.4	0.0949	1.8	.512	
5.1	0.0609	2.7	10.4	1.7	0.0584	3.5	0.775	3.9	0.0962	1.7	.441	
6.1	0.0591	2.7	10.83	1.7	0.0591	2.7	0.752	3.2	0.0923	1.7	.526	
7.1	0.0599	2.1	10.72	1.5	0.0599	2.1	0.771	2.6	0.0933	1.5	.580	
8.1	0.06339	1.5	9.94	1.4	0.0611	2.3	0.848	2.7	0.1006	1.4	.529	
9.1	0.06112	0.9	9.74	1.2	0.06055	0.98	0.857	1.6	0.1026	1.2	.779	
10.1	0.06088	1.4	9.43	1.3	0.06088	1.4	0.89	2	0.106	1.3	.689	
11.1	0.06077	1.1	9.79	1.3	0.06077	1.1	0.856	1.7	0.1022	1.3	.774	

Errors are 1 – sigma; Pb_c and Pb^* indicate the common and radiogenic portions, respectively.

Error in standard calibration was 0.56% (not included in above errors but required when comparing data from different mounts).

(1) Common Pb corrected using measured ^{204}Pb .

zircons were extracted from the sample and consisted of elongate prismatic grains with oscillatory zoning. Some grains had clearly identifiable rims and embayments resulting from secondary recrystallisation and growth (e.g. grain 4 Fig. 11). A total of 15 zircons were analysed. Data from the oscillatory zoned cores ($n=8$) provide a concordant age of 637 ± 5 Ma (Fig. 12b). This is interpreted as the crystallisation age of the Ramiane Suite. Garnet development in this granite appears to post-date the crystallisation of the granite and the chemistry of the garnet is not consistent with crystallisation from a primary magma (Karlsson, 2006). The garnet is therefore interpreted to have formed during a later high pressure metamorphic event and this event was associated with the formation of the rims and embayments described above. The data from the metamorphic rims and embayments yield an age of 596 ± 5 Ma ($n=4$) (Fig. 12b). Six analyses were either discordant or fell between the two populations and were not included in the calculation of ages.

6.2. Metachéria Metamorphic Complex (two pyroxene mafic garnet granulite JM05MC14)

Sample JM05MC14 is a weakly banded mafic granulite. Zircon is not abundant within the sample and only a small amount of zircon was recovered. From these recovered zircons two populations could be identified. The first population is made up of smaller idiomorphic acicular grains with oscillatory zoning whereas the second population has homogeneous cathodoluminescence (little if any zoning), low U content and an angular grain shape. A total of 12 spots were analysed from 11 zircons. The first group of grains ($n=6$) provided a concordant age of 634 ± 8 Ma whereas the second group ($n=4$) yielded a concordant age of 579 ± 11 Ma (Fig. 12a). One point (point 3.1) was highly discordant and was not included in the calculation of ages. A second point (point 2.2) was a core of one of the smaller idiomorphic grains and yielded an older $^{207}\text{Pb}/^{206}\text{Pb}$ age of 727 ± 41 Ma (Table 3). These data have been previously referred to as a crystallisation age (~635 Ma) and a younger metamorphic age (~579 Ma) (Grantham et al., 2007, 2008). However, assessment of the Th/U ratios (Fig. 13) indicates that the formation of the zircon grains may be ambiguous as both groups of zircon have comparably low Th/U ratios generally taken to indicate metamorphic zircon growth (Rubatto, 2002). Furthermore, there is clear field evidence that the Ramiane Pluton is intrusive into the Metachéria Metamorphic rocks at ~637 Ma and it would therefore be difficult to envisage the 634 Ma age being crystallisation of the igneous precursors to the



Fig. 14. Field photo showing the Ramiane Pluton with a large xenolith of foliated intermediate (hornblende bearing) granulite.

metamorphic rocks. Moreover, foliated xenoliths of the Metachéria Metamorphic rocks are found within the Ramiane Pluton (Fig. 14) indicating that the Metachéria rocks must have been emplaced and deformed prior to intrusion of the Ramiane Suite. We therefore suggest that the 634 Ma age represents a metamorphic age and that the slightly older ages recorded in some cores (i.e. the ~727 Ma age) may represent the age of crystallisation of the igneous protoliths to the banded granulitic rocks. The 579 ± 11 Ma date may also be a metamorphic age related to progressive exhumation of the rocks during the main Gondwana collisional phase.

7. Metamorphism and structural history

Structurally and metamorphically the Monapo Klippe is distinct from the surrounding Nampula Block gneisses. It is surrounded at its margin and base by a strong zone of mylonitised gneiss which has contributed to its interpretation as a klippe structure (Pinna et al., 1993; Pinna, 1995). This is supported by the distinctly different geochronology derived from rocks within the klippe as compared to within the Nampula gneisses along with differences in metamorphic grade. Granulite-facies metamorphic assemblages in mafic gneisses (garnet + clinopyroxene + orthopyroxene) and in pelitic rocks (sillimanite + garnet + K-feldspar) attest to the high temperature and pressure conditions of metamorphism. Grantham et al. (in press) has estimated peak conditions to be in excess of 10 kb at temperatures of ~900 °C. This was followed by isothermal decompression resulting in hornblende + plagioclase and clinopyroxene + plagioclase symplectites on garnets in mafic lithologies. This exhumation of the high-pressure assemblage to mid-crustal levels was associated with isobaric cooling and hydration at between ~4–7 kb and 550–700 °C (Grantham et al., in press). Hydration is manifested in the widespread development of hornblende ± biotite in various lithologies. The timing of granulite-facies metamorphism is linked to the 634 ± 8 Ma age recorded in the Metachéria mafic granulite. In the Ramiane Pluton, garnets have andraditic compositions and plagioclase is albitic (An_{70–85}) (Karlsson, 2006) suggesting that the garnet has formed as a result of metamorphism with calcic-plagioclase breakdown contributing to the formation of elevated grossular contents in the garnet. The timing of this event is linked to the 596 ± 5 Ma age in the Ramiane Suite. The 579 ± 11 Ma age of metamorphism in the Metachéria just barely post-dates the 596 ± 5 Ma metamorphic ages in the Ramiane Suite, possibly recording a diachronous metamorphic response by different lithologies (consistent with zircon growth continuing to lower temperature in the Metachéria following peak metamorphism). More work is needed to definitely clarify the timing of

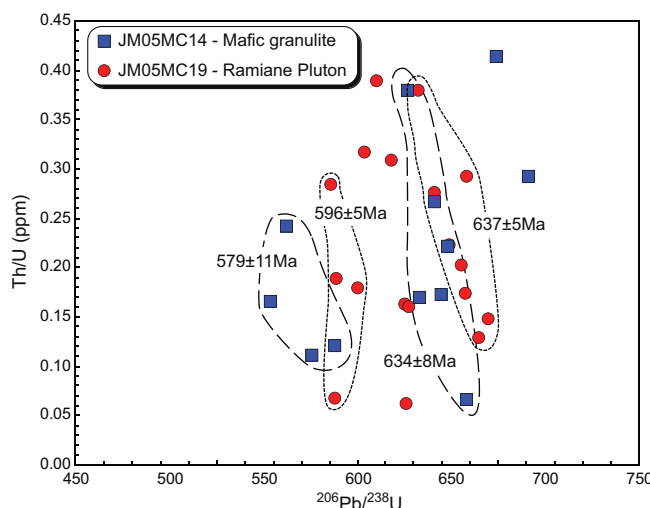


Fig. 13. Variation of Th/U ratio with $^{206}\text{Pb}/^{238}\text{U}$ age showing the lack of clarity in metamorphic versus igneous Th/U ratio of analysed zircon grains.

events in these rocks. Locally in the uppermost footwall to the Klippe, trace amounts of garnet have been identified in biotite-rich gneisses of the Mamala/Molócué Groups and Culcui Suite. Garnet is not observed elsewhere in these Nampula Block lithologies and this is therefore potentially indicative of a metamorphic aureole related to overthrusting by the granulitic nappe.

The Monapo Klippe has four main structural elements associated with it. These are: (1) a damage zone in the underlying footwall gneisses; (2) the marginal mylonite; (3) structural elements including shear fabrics within the klippe that likely predate its emplacement; and (4) the current basin-shaped geometry of the klippe which resulted from post-emplacement horizontal constriction. The distributed ductile damage zone observed in the footwall (Nampula gneisses) to the Monapo Klippe contains planar and linear shear fabrics with similar orientations to those of the marginal mylonite. The shear fabrics in the highly localised mylonite, including the deformation of late pegmatitic intrusions, are characteristic of quartz-ductile, feldspar-brittle conditions typical of greenschist-facies and support an interpretation of effective progressive exhumation of the base of the nappe during emplacement. These originally planar lineations now have moderate to steep dips in both an east and west orientation. Lineations and shear fabrics measured within the Monapo Klippe do not match those of the footwall and marginal mylonite. They are generally far more variable in both their orientation and dip and this is likely due to the inheritance of internal shear fabrics in the complex which predate the juxtaposition of the complex against the Nampula Block.

As the regional Nampula Block gneisses are generally unstratified and are highly deformed, the Monapo mylonite itself represents the most coherent surface in the region that was approximately planar and continuous during final emplacement. The steeply plunging motion indicators and shear lineations oblique to the dip of the foliation require folding of the mylonite, and the region generally, subsequent to the emplacement of the thrust sheet. Beginning with the assumption that the original geometry of the basal shear zone would have been more planar than it is in present day, and that the shear and stretching lineations would have been roughly parallel on the scale of the current complex exposure (~40–50 km) some constraints on post-assembly folding can be established. First, the steeply dipping fabrics on the east and west side of the complex suggest a regional synclinorium with a doubly plunging north-south trending axis. North-south trending fold axes were inferred in the Nampula Complex within the area by Grantham et al. (2007) on the same order scale as those interpreted to fold the Monapo Klippe. In general, to restore the Monapo marginal mylonite to regional uniformity requires rotations on the order of 60°, so the regional folding may have accommodated ~100% shortening. However, the doubly plunging fold geometries are not easily explained by stepwise rotation so a regional interference fold field creating 10 s km scale basins and domes is the preferred model. Similar doubly plunging folds were described on regional to outcrop scales by Viola et al. (2008) in the Cabo Delgado Nappe Complex to the north as well as by Ueda et al. (2012) for the northern Nampula Block and interpreted as interference folds. East-vergent extension was documented by Viola et al. (2008) and attributed to post-orogenic collapse. The folding of the Monapo mylonite provides evidence of postemplacement horizontal constriction, suggesting that the deformation took place during late stage compression of the Malagasy/Kuunga Orogeny. Internal to the Monapo Klippe, the regional interference folding overprints earlier structural features (implied by the curvilinear lithologic boundaries forming the mushroom-like shape in the eastern half of the complex, Fig. 2a). Grantham et al. (2007) also described the curving fold axes and attributed them to a two-stage interference folding process. We suggest that a simpler explanation would be the development of overturned to sheath-like fold structures during intense

shear strain at the base of the granulite nappe (Fig. 2b). The general westward dip of internal fabrics and the “mushroom” shapes reported by Grantham et al. (2007) in geophysical observations of the complex would be explained by overturned, east-vergent folds including a larger antiform in the east where the rigidity of the Ramiane Suite intrusives affected fold scale. This type of fold geometry is common where basal drag produces folding in the hanging wall of a sub-horizontal thrust sheet (Boulier et al., 1978). This model accommodates the dissimilar curvature of the inferred fold axes and extreme thinning of interleaved Monapo Klippe lithologies on the limbs of the folds better than the model which requires multiple scales and orientations of interference folding. It is also consistent with earlier work associating the Monapo Klippe with the Ocua Complex of the Lúrio Belt as tectonic mélange. We thus suggest that much of the complicated internal structure of the Monapo Klippe on the sub-10 km scale formed by shear and overturning at the base of nappe emplacement but that the macroscopic structural bowl (doubly-plunging synclinorium on 10 s km-scale) where the complex is preserved today is a result of post-emplacement horizontal constriction in the core of the orogen.

8. Discussion

8.1. Origin of the Metachéria Metamorphic Complex lithologic assemblage

The intimate interleaving of mafic and metasedimentary rock types on a range of scales from 100 s m to 10 s cm justifies the description of the Metachéria Complex as a mélange terrane. There are two end-member models for tectonic history: one in which the mixing of rocks occurred syn-depositionally and one in which all interleaving is tectonic in origin. Although both will be discussed, we prefer a hybrid model whereby primary lithostratigraphic complexity is amplified by tectonic shearing. Low fabric intensity in the Mazerapane and Ramiane Suites, and the depth and age of emplacement consistent with peak metamorphism of the Metachéria Complex, demonstrate that the Metachéria was well developed structurally during or prior to burial. Outcrop patterns and weak fabrics imply that the Monapo assemblage was complete prior to final emplacement atop the Nampula Block. This is supported by the inverted thermal architecture and the association of final shearing on the boundary with Neoproterozoic granitic intrusions.

In order to interpret the origins of the klippe, some interpretations as to the likely protoliths of the lithologies present must be made. Some of the lithologies are clearly metasedimentary in origin. The kyanite-sillimanite bearing rocks are pelitic while the carbonates represent limestones. The mafic granulites which form a major unit of the Metachéria Metamorphic Complex are geochemically consistent with basalt or gabbro of E-MORB affinity while the slightly elevated LREE of the intermediate granulites, which are hornblende-bearing, suggests an island-arc affinity. The lack of a pronounced Nb-Ta anomaly however, argues against a strong island-arc component. Intercalated ocean-floor basalts and deep to shallow marine sediments are characteristic features of terranes formed by obduction of oceanic crust, such as ophiolites and some tectonic nappes found in accretionary wedge complexes. The dominance of mafic to intermediate igneous rocks over meta-sediments is reminiscent of the lithostratigraphy of an oceanic plateau or an oceanic spreading ridge in a marine basin which has some terrigenous sediment input.

Most of the mafic to intermediate rocks in northern Mozambique, both north and south of the Lúrio Belt, are probably related to the Mozambique Ocean which was consumed during

the convergence of central Gondwana between 650 and 490 Ma. The closure of this ocean was associated with accretion of various volcanic arc and microcontinent fragments onto the margin of the Congo-Tanzania Craton between 655 and 610 Ma (Meert, 2003; Collins and Pisarevsky, 2005; Jöns and Schenk, 2008; Bingen et al., 2007). Oceanic spreading ridges that existed between these components are therefore a likely source for the parental materials that make up the Monapo Klippe. This is consistent with similar terranes nearby such as the Eastern Granulites in Tanzania and the Vohibory Complex in Madagascar (Collins et al., 2012; Jöns and Schenk, 2008), which have similar lithological packages to the Monapo Klippe, and are inferred to represent fragments of island arc complexes (as summarised by Bingen et al., 2009). Accretion and the associated stacking of tectonic slices during closure and subduction and/or obduction of the Mozambique Ocean created the current amalgamation of rock units in the Monapo Klippe which were subsequently intruded by the Ramiane and Mazerapane Suite rocks.

8.2. Emplacement of the Ramiane and Mazerapane Suites

Comparison of the geochronology data from the Ramiane Suite and the Metachéria Metamorphic Complex indicates that the Ramiane Suite rocks intruded at mid to lower crustal levels synchronously with granulite-facies metamorphism (~635–637 Ma). The alkali character of the granites further means that the granitic rocks would have been well out of equilibrium with the metamorphic rocks, none of which contain significant amounts of K (Supplementary Table S1). This probably accounts for the pronounced K-fenitisation halo that exists around the Ramiane Suite rocks (Fig. 2c), where intrusion of the Ramiane rocks caused K-metasomatism into the surrounding country rocks. Such metasomatism also would have generated migmatisation in the country rocks which accounts for the variable migmatitic character of the nearby rocks. Field observations indicate that these plutons are built up as sheets. This, in part, accounts for the extremely elongate and thin bands of leucogneiss/leucopegmatite that occur outside of the main plutonic bodies in the west (Fig. 3). The current geometry of the Ramiane Suite rocks (Fig. 3) may be the result of overturned to sheath-like fold structures that developed in response to intense shear strain at the base of the granulite nappe when the nappe was being emplaced.

In comparison to the Ramiane Suite, much less is understood about the intrusion of the Mazerapane Suite rocks. Their ultramafic character and silica-undersaturated nature indicates that they are totally distinct from the Ramiane Suite Rocks. No cross-cutting relationships were seen in the field and there does not appear to be any form of metasomatic alteration or contact metamorphic halo associated with their intrusion. Given their ultramafic character, they would have intruded at significant temperatures, certainly high enough to generate a contact metamorphic overprint in the country rocks. The apparent absence of this suggests that the Mazerapane Suite rocks also intruded during the granulite-facies metamorphism. In contrast to the Ramiane Suite rocks though, some components of the Mazerapane Suite rocks have strong fabrics developed. Although these fabrics are interpreted to be dominantly tectonic in origin, in places they continue a short distance into the pegmatoidal zones of the nepheline syenite for example (see Fig. 5c), suggesting that some of these rocks (i.e. the nepheline syenite) were not fully crystallised when the fabric was developing. Deformation must have been ongoing after peak metamorphism, as the nepheline syenite shows evidence of syn-deformational replacement of clinopyroxene by biotite which could not have happened at granulite-facies.

8.3. Correlations with other granulite terranes and implications for Gondwana assembly

The correlation of granulite-facies rocks throughout central Gondwana has underpinned the concept of a regionally extensive mid- to lower-crustal mega-nappe sheet developed during Gondwana assembly (e.g. Pinna et al., 1993; Viola et al., 2008; Grantham et al., 2008, *in press*). Granulite-facies terranes cited as potentially forming part of this mega-nappe sheet include the Eastern Granulites Tanzania, the Highlands Complex Sri Lanka, the Vohibory Complex Madagascar, the Urungwe Klippe in Zimbabwe, the Mavhuradonha Complex and Masosa Suite in NE Zimbabwe, the NE Sør Rondane and Schirmacher Hills Antarctica. This also includes the Cabo Delgado Nappe Complex, comprising the Xiano, Muaquia, M'Sawise and Lalamo complexes as well as the Ocua Complex rocks that mark the boundary between the Nampula and Namuno Blocks. The lithologic, metamorphic and geochronologic characteristics of, and potential correlations between, these terranes has been summarised in Table 4.

The most important of these is the presence of a distinct metamorphic event at ca. 630 Ma which is present in some of the above terranes but not all. ~630 Ma ages have been previously reported in terranes that are largely distal to NE Mozambique, principally the Eastern Granulites (641 ± 1 Ma, Muhongo et al., 2001), the NE Sør Rondane and Schirmacher Hills in Antarctica (ca. 630 Ma and 632 ± 8 Ma respectively; Grantham et al., *in press*; Ravikant et al., 2008) and the Vohibory Complex (638 ± 25 Ma, Jöns and Schenk, 2008). This is significant in that it implies that the 630 Ma high-grade metamorphic event in the Monapo Klippe was associated with the EAO, and underlines the truly allochthonous nature of the klippen complex that could not have been in its current position given the absence of the 630 Ma metamorphism in the underlying Nampula gneisses. Likewise the Cabo Delgado Nappes in the Namuno Block north of the Lurio Belt, show evidence of a high-grade metamorphic overprint at ca. 630 Ma (see Table 4) that is not recorded in the underlying Unango and Marrupa Complexes. These two Mesoproterozoic (~1060–940 Ma) (Fig. 1) complexes only experienced an amphibolite (Marrupa Complex) to lower granulite-facies (Unango Complex) metamorphism at 555 and 570–530 Ma, respectively (Bingen et al., 2009). An identical timing of high-grade metamorphism of 560–540 Ma is indicated for the Ocua Complex rocks that delineate the Lurio Belt (Bingen et al., 2009). These results suggest that the burial and high-grade metamorphism of the accreted arcs and oceanic crust together with terrigenous sediments occurred during the later stages of the EAO at ca 630 Ma and prior to the convergence of the Namuno and Nampula Blocks between ca. 590 Ma and 550 Ma (Grantham et al., *in press*). The top to the W and WNW kinematics recorded in the thrust stack of the Namuno Block formed during this terminal phase of the EAO (Viola et al., 2008; Bingen et al., 2009).

This process must have taken place in two phases, the first of which generated high-grade metamorphism in the Cabo Delgado Nappes and the second generating the imbricate nappe stack that characterises the Namuno Block. The Kalahari and Congo-Tanzania cratons were located to the west of these accreted terranes. It is conceivable that the final accretionary stages in the EAO that record east-west convergence (Meert, 2003) resulted from locking up of the accretionary stack against these cratons. This locking up process caused a swing in the direction of crustal convergence from a dominantly east-west direction (collision of Azania with the Congo Craton) to a dominantly north-south direction that facilitated the second phase of crustal convergence associated with the Malagasy Orogeny (India colliding with the above amalgam at ~570–500 Ma; Collins and Pisarevsky, 2005). Progressive transpressional shearing during the later stages of convergence resulted in the piggy-back thrusting of the already imbricated Unango, M'Sawise, Muaquia,

Marrupa, Xixano, Nairoto and Lalamo complexes over the Nampula Block. The latter was, at this time, likely contiguous with the western parts of the East Antarctic Craton, i.e. Maud Belt of Western Dronning Maud Land (Grantham et al., 2008, in press) and therefore still peripheral to the Kalahari Craton. During the initial convergence, relics of the Mozambique Ocean were obducted forming the ophiolitic slivers of the Ocua Complex. These slivers, in turn, were subsequently overridden by the Namuno Block imbricate stack and metamorphosed to granulite-facies grades at ca. 560–530 Ma (Engvik et al., 2007; Grantham et al., 2008). Likewise the Nampula Block gneisses record metamorphism between 555 and 502 Ma (Bingen et al., 2009; Macey et al., 2010; Thomas et al., 2010).

In the above model, the Monapo Klippe, like the nearby Mugeba Klippe, represents a remnant of the overriding Namuno Block imbricate stack and specifically a slice of the Cabo Delgado Nappe. Its isolated outcrop appearance is attributed to the high of erosion in Africa, with more extensive preservation of this mega-nappe found in Antarctica where the total exhumation by erosion is significantly less (Grantham et al., in press), hence the link with the rocks of the Schirmacher Oasis and the NE Sør Rondane (Table 4). The absence of any of the Marrupa or Unango allochthons between the Monapo and the underlying Nampula Gneisses indicates the lateral variability of these crustal slivers, either due to primary lithological heterogeneities or due to the truncation of units along the basal

thrust. Unfortunately, the post-emplacement refolding and recrystallization of textures of rocks of the Monapo Klippe complicate the interpretation of stretching lineations and kinematic indicators that could be related to the actual emplacement of the klippe.

8.4. Timing of emplacement of the Monapo Klippe

The Monapo Klippe was brought to its current position either during the progressive thrusting of the Namuno mega-nappe over the Nampula-Maud Block (Grantham et al., in press) or during post-collisional extensional collapse of the thickened crust that resulted from the combined EAO and Malagasy orogenies (Ueda et al., 2012). In either case, the timing of emplacement is given by detrital zircon ages that constrain the deposition of the coarse-clastic, intramontane sediments of the Mecubúri Group in small, fault-bounded foreland basins of the advancing Unango + Marrupa + Cabo Delgado imbricate stack to ca. 530 Ma (Thomas et al., 2010), implying the klippe could only have been brought to its current position at this time.

The post-emplacement (i.e. 530 Ma or younger) folding of the Monapo Klippe is probably linked to the fact that post-collisional extensional collapse of the thickened crust occurred in an environment where the boundaries of the extensional collapse are pinned by the positions of the Congo-Tanzania, Kalahari and East Antarctica cratons. In this environment extensional collapse should

Table 4
Comparison of the lithologic, metamorphic and geochronologic character of the Monapo Klippe in comparison to other isolated granulitic outcrops throughout central East Dirks and Jelsma, 2006; Hargrove et al., 2003; Melezhik et al., 2008; Stagman, 1962; Gondwana.

	Monapo Klippe	Mugeba Klippe	Ocua Complex	Xixano Complex	Muaquia Complex	M'Sawise Complex	Lalamo Complex
	<i>This study</i>	<i>Roberts et al. (2005) Kroner et al. (1997)</i>	<i>Engvik et al. (2007) Viola et al. (2008)</i>	<i>Boyd et al. (2010) Melezhik et al. (2008)</i>	<i>Viola et al. (2008) Boyd et al. (2010)</i>	<i>Viola et al. (2008) Boyd et al. (2010)</i>	<i>Viola et al. (2008) Boyd et al. (2010) Melezhik et al. (2008)</i>
LITHOLOGIES	Similar Lithologies	Granitic and syenitic gneisses	Charnockite granulites	Granitic and syenitic gneisses	Granitic gneiss	Granitic gneiss	Granitic to granodioritic gneiss
				Tonalitic and dioritic gneiss	Opx-bearing tonalitic gneisses	Tonalitic gneiss	Tonalitic gneiss
				Quartz-feldspar gneiss	Quartz-feldspar gneiss		
				Mylonitic leucogneiss		Banded migmatitic gneiss	
		Nepheline syenite					
		Pyroxenite	Pyroxenite				
		Metagabbro			Amphibolitic-dioritic gneiss	Gabbroic and amphibolitic gneiss	Metagabbro
METAMORPHISM	Disimilar lithologies						
		Marginal mylonite	Marginal mylonite				Meta-conglomerate
					Mica schist		Mica schist
							Quartzite
					Metasandstone		Metasandstone
GEOCHRONOLOGY	Metamorphic				Meta-rhyolite		
		Granulite	c. 10 kbar c. 900 to 1000 °C Isothermal decompression	c. 10 kbar c. 900 to 1000 °C Isothermal decompression	15.7 ± 1.4 kbar 949 ± 92°C Isothermal decompression	Preserved in tectonic lenses	Early high pressure metamorphism
		Amphibolite / Retrogression	c. 6 - 7 kbar c. 700 °C Isobaric cooling	c. 6 - 7 kbar c. 700 °C Isobaric cooling		Paragneisses only	Main event amphibolite-facies
		Intrusive/ Crystallisation	637 ± 7 Ma 635 ± 3 Ma			818 ± 10 Ma 744 ± 11 Ma	
		Deposition				850 - 740 Ma	622 ± 9 Ma
TECTONIC SETTING	Metamorphic						696 ± 13 Ma
		Metamorphic	596 - 579 Ma	615 ± 7 Ma	557 ± 16 Ma (Zr) 540 ± 7 Ma (Mon)	735 ± 4 Ma 631 ± 6 to 607 ± 11 Ma	740 Ma (marbles)
		Thrust klippe separated from underlying Nampula Block by mylonite of variable thickness	Thrust klippe separated from underlying Nampula Block by mylonite of variable thickness	Possible tectonic melange concentrated in high strain zone (suture) separating the Nampula Block from the Unango Complex	Part of the Cabo Delgado Nappe Complex. Structurally overlies the lower grade Marrupa and Nairoto complexes by major shear zones	Structurally overlies the Marrupa Complex and forms part of the Cabo Delgado Nappe Complex	Overtakes and almost enclosed by Marrupa Complex and forms part of the Cabo Delgado Nappe Complex
							Overtakes the Nairoto and Meluco complexes and is itself overlain by the Rovuma basin. Part of the Cabo Delgado Nappe Complex with most boundaries tectonised

Table 4 (Continued)

		Highland Complex Sri Lanka	Eastern Granulites Tanzania	Vohibory Complex Madagascar	Urungwe Klippe Zimbabwe	Mavuradonha Complex and Masosa Suite NE Zimbabwe	NE Sor Rondane Antarctica	Schirmacher Hills Antarctica
		Sajeet et al. (2007) Holz et al. (1994)	Muhongo and Lenoir (1994) Muhongo et al. (2001)	Jons and Schenk (2008)	Stagman (1962) Vail and Snelling (1971)	Hargrove et al. (2003) Dirks and Jelmsa (2006)	Grantham et al. (2012)	Grantham et al. (2012) Ravikant (2006) Ravikant et al. (2008)
LITHOLOGIES	Similar Lithologies	Charnockitic granitic gneisses		Granitic gneisses	Granitic gneisses		Charnockitic gneisses	Quartzofeldspathic augen gneiss
		Opx-bearing tonalitic gneisses						Opx-bearing tonalitic gneisses
		Migmatitic gneiss					Migmatites	
					Banded ironstones			
				Serpentinites	Serpentinites	Harzburgite and pyroxenite	Minor pyroxenite and websterite	
					Meta-arkose			
			Anorthosites			Anorthosite		Gabbroic anorthosite
		Homblende gneiss	Metabasic rocks	Amphibolites			Metagabbro	Metagabbro
						Mylonite		
						Meta-volcanic or mylonitic		
METAMORPHISM	Dissimilar lithologies	Quartzite	Migmatitic gneisses					
GEOCHRONOLOGY	Granulite	c. 12.5 kbar c. 925 °C HP-UHT	8 - 12 kbar 800 - 900 °C	9 - 12 kbar 750 - 880 °C High pressure metamorphism		10 - 11 kbar c. 880 - 900 °C Decompression	10 kbar (at least) 900 °C	8 ± 1 kbar 800 ± 50 °C
	Amphibolite / Retrogression	Retrograde amphibolite facies overprint					6 - 7 kbar 600 - 700 °C Retrogression	5 ± 1 kbar 700 ± 50 °C Isothermal decompression
	Intrusive/ Crystallisation	1.85 - 1.9 Ga	Neo- to Mesoproterozoic and older emplacement ages	850 - 700 Ma	732 ± 20 to 1008 ± 63 Ma (K-Ar)	795 ± 2 Ma, 870 ± 5 Ma 1052 ± 14 Ma	Late Mesoproterozoic	800 - 1150 Ma
TECTONIC SETTING	Deposition	1.9 - 2.0 Ga	700 - 745 Ma detrital zircon age in metapelites					
	Metamorphic	c. 580 Ma	641 ± 1 Ma	638 ± 25 Ma (Mon) 612 ± 5 Ma (Zr)	500 Ma (K-Ar)	550 - 530 Ma	~630 Ma to ~530 Ma with 5 metamorphic pulses defined	632 ± 8 Ma
			Allochthonous nappes overlying Archaean to Palaeoproterozoic felsic crust of the Congo-Tanzania Craton	Formed as an arc-terrace and associated back-arc basin at the margin of the Neo-Mozambique Ocean and then accreted onto the margin of the microcontinent Azania		Allochthonous rocks thrust-faulted southwards onto the N. margin of the Zimbabwe Craton		

generate normal faulting and high erosion rates in the orogenic core and thrust faulting and sedimentary deposition in the foreland (e.g. Rey et al., 2001; Selverstone, 2005). The synchronous generation of normal and thrust faulting in such an environment could explain the presence of both late compressional and extensional fabrics documented by Ueda et al. (2012) to overprint the main ~550 Ma collisional fabric. Similarly the presence of both compressional and extensional fabrics has likely contributed to the ambiguity of kinematic indicators in and around the Monapo Klippe. Further work on resolving these features is necessary to resolve unambiguously the exact transport direction and path of the Monapo Klippe.

Acknowledgements

Much of this work was carried out as part of the Mineral Resources Management Capacity Building Project of the Ministry of Mineral Resources of Mozambique and funded by the World Bank and the South African Government. The mapping and research was implemented by teams from the Council for Geoscience of South Africa (CGS) and the National Directorate of Geology of Mozambique. Additional mapping and research was undertaken by the University of Stellenbosch and the University of Cape Town and funded through the National Research Foundation. The paper is being published with the permission of the National Directorate for Geology, Maputo and the Executive Officer of the CGS. CR and JM acknowledge support by the South African National Research Foundation grant FA2007033000013 and JM acknowledges additional funding from Subcommittee B at Stellenbosch

University. JM and CR thank L. Rudd, M. Webster, J.F.A. Diener, and T. Dhansay for contributions and discussions in the field, the field assistance of Dr. Michequé from the Nampula DNG office and PM acknowledges the field assistance of C.F. Camillo. Discussions with G. Stevens helped to clarify some of the ideas presented in the manuscript and comments by A. Kisters on an earlier version of the manuscript significantly improved it. We thank A. Collins and J. Jacobs for constructive reviews that helped to clarify and improve the manuscript.

Appendix 1. Analytical techniques

Major, trace and REE geochemistry

Whole rock powders for determining major, trace and REE compositions were prepared at the Pretoria laboratory of the Council for Geoscience in South Africa and then sent to the ICP Laboratory at Royal Holloway, University of London for analysis using ICP-AES and ICP-MS techniques. For ICP-AES analysis, 0.2 g of powdered sample was dissolved in 6 ml of a 2:1 mixture of HF and HClO₄. The solution was then evaporated to dryness, cooled and dissolved in 20 ml of 10% HNO₃. This solution was analysed by ICP-AES for a suite of elements including Fe, Mg, Ca, Na, K, Ti, P, Mn, Ba, Ce, Co, Cr, Cu, La, Li, Ni, Pb, Sc, Sr, V, Y and Zn. The lithium metaborate fusion-dissolution involves the fusion of 0.2 g of powdered sample with 1 g of LiBO₂ at 950 °C and the mixture dissolved in 5% HNO₃. The solution was then analysed for a suite of major elements including Si, Al and Zr by ICP-AES and a suite of trace and rare earth elements by

ICP-MS. To achieve high precision ICP-AES analysis (reproducibility better than 0.5%) a lithium metaborate flux (prepared in-house) containing 1% Ga_2O_3 was used. Drift monitors were run at regular intervals to measure and correct for any instrumental drift. All analyses were made using the Perkin Elmer Optima 3300R ICP-AES system and the Perkin Elmer 5000 ICP-MS instrument. Working detection limits for ICP-AES are 5 ppm for Ba, 4 ppm for Zr and Ni and 2 ppm of pr Co, Cr, Cu, Li, Sc, Sr, V, and Zn. For ICP-MS the working detection limits are 1 ppm for Rb, Nb, Y, La, Ce, Pr, Nd, Sm, As, and Pb, 0.5 ppm for Gd, Ag, and Sn, 0.2 ppm for Eu, Dy, Ho, Er, Yb, Cd, Tl, Mo, Sb and Bi and 0.1 ppm for U, Th, Cs, and Lu.

SHRIMP geochronology

Zircons were extracted from whole-rock samples by Elijah Nkosi at the laboratories of the CGS in Pretoria following standard separation techniques making use of sieves, the Wilfley percussion table, the Frantz magnetic separator and heavy liquids. The zircon concentrates were examined under a binocular microscope and suitable grains were mounted in epoxy, together with the zircon reference FC1 (Duluth Gabbro). Photomicrographs in transmitted and reflected light were taken of all of the zircons and these, together with scanning electron microscope (SEM) cathodoluminescence (CL) images, were used to determine the internal structures of the sectioned grains and to target specific areas (e.g. core). The zircon epoxy mounting, photographing and CL imaging was completed at the Research School of Earth Sciences (RSES) at the Australian National University (ANU) in Canberra. The U-Pb-Th analyses of were completed using the Sensitive High Mass Resolution Ion Microprobe (SHRIMP) II and SHRIMP RG (spot diameter of c. 20 μm) at the ANU RSES. The age of crystallisation and metamorphism of igneous rock samples was determined by analysing approximately twenty spots for each sample and six scans through the requisite mass range per spot. The age determinations of detrital zircons of meta-sedimentary rocks involved analysing more than 50 grains with five scans through the requisite mass range per spot. Counting times for each isotope analysed are listed in the table below. The standard (FC1) was analysed between the analyses of every two or three unknown zircon samples.

Isotope counting times		
Isotope	Counting time crystallisation	Counting time detrital
^{196}Zr	2	2
^{204}Pb	10	10
204.1 (background)	10	10
^{206}Pb	15	15
^{207}Pb	30	40
^{208}Pb	10	5
^{238}U	5	7
^{248}Th	2	3
^{254}UO	2	2

The data have been reduced by employing methods similar to those described by Williams (1998, and references cited within), and using the SQUID Excel Macro of Ludwig (2000). For the zircon calibration, the Pb/U ratios have been normalised relative to a value of 0.1859 for the $^{206}\text{Pb}/^{238}\text{U}$ ratio of the FC1 reference zircons, equivalent to an age of 1099 Ma (Paces and Miller, 1989). Common Pb was corrected for using the measured ^{204}Pb . U and Th concentrations were determined relative to the SL13 standard. Uncertainties given for individual analyses (ratios and ages) are reported at the 1σ level, however uncertainties in the calculated weighted mean ages are reported as 95% confidence limits. The concordia plots and weighted mean age calculations were carried out using Isoplot/Ex (Ludwig, 1999).

References

- Bingen, B., Viola, G., Griffin, W.L., Jacobs, J., Boyd, R., Thomas, R.J., Daudi, E., Henderson, I.H.C., Beyer, E., Skar, Ø., Engvik, A., Key, R.M., Solli, A., Sandstad, J.S., Smethurst, M., Tveten, E., Bjerkgård, T., Melezihik, V.A., Jamal, D., Smith, R., Hollick, L.M., Feito, P., 2007. Crustal architecture of the Mozambique Belt in northeastern Mozambique: perspective from U-Pb geochronology and Lu-Hf isotopes in zircon. In: 7th International Symposium on Applied Isotope Geochemistry, Stellenbosch, 10–14 September.
- Bingen, B., Jacobs, J., Viola, G., Henderson, I.H.C., Skar, O., Boyd, R., Thomas, R.J., Solli, A., Key, R.M., Daudi, E.X.F., 2009. Geochronology of the Precambrian crust in the Mozambique Belt in NE Mozambique and implications for Gondwana assembly. *Precambrian Research* 170, 231–255.
- Boger, S.D., Wilson, C.J.L., Fanning, C.M., 2001. Early Paleozoic tectonism within the East Antarctic craton: the final suture between east and west Gondwana. *Geology* 29, 463–466.
- Boulier, A.M., Davidson, I., Bertrand, J.-M., Coward, M.P., 1978. L'unité granulitique des Iforas: une nappe de socle d'âge Pan-Africain pré-coe. *Bulletin de Société Géologique Francaise* 20, 877–882.
- Boyd, R., Nordgulen, O., Thomas, R.J., + 23 others, 2010. The geology and geochemistry of the East African Orogen in northeastern Mozambique. *South African Journal of Geology* 133, 87–129.
- BULGARGEOIN (B.R.G.M.), 1984. Jazigo de apatite de Evate: resultados da pesquisa preliminary executada em 1981–1983, Maputo.
- Collins, A.S., Pisarevsky, S.A., 2005. Amalgamating eastern Gondwana: the evolution of the Circum Indian Orogens. *Earth Science Reviews* 71, 229–270.
- Collins, A.S., Kinnny, P.D., Razakamanana, T., 2012. Depositional age, provenance and metamorphic age of metasedimentary rocks of southern Madagascar. *Gondwana Research* 21, 353–361.
- Collins, A.S., Santosh, M., Braun, I., Clark, C., 2007. Age and sedimentary provenance of the southern granulites, South India. *U-Th-Pb SHRIMP secondary ion mass spectrometry*. *Precambrian Research* 155, 125–138.
- Dirks, P.H.G.M., Jelsma, H.A., 2006. The structural-metamorphic evolution of the northern margin of the Zimbabwe Craton and the adjacent Zambezi Belt in northeastern Zimbabwe. *Geological Society of America Special Paper* 405, 291–313.
- Eby, G.N., 1992. Chemical subdivision of the A-type granitoids: petrogenetic and tectonic implications. *Geology* 20, 641–644.
- Engvik, A.K., Tveten, E., Bingen, B., Viola, G., Erambert, M., Feito, P., de Azavedo, S., 2007. P-T-t evolution and decompression textures of Pan-African high-pressure granulites, Lúrio Belt, northeastern Mozambique. *Journal of Metamorphic Geology* 25, 935–952.
- Grantham, G.H., Macey, P.H., Ingram, B.A., Roberts, M.P., Rohwer, M., Opperman, R., Manhica, V., Alvares, S., Bacalhau, Du Toit, M.C., Cronwright, M., Thomas, R.J., 2007. Map Explanation Sheets Meconte (1439) and Nacala (1440) National Directorate of Geology, Republic of Mozambique.
- Grantham, G.H., Macey, P.H., Ingram, B.A., Roberts, M.P., Armstrong, R.A., Hokada, T., Shiraishi, K., Jackson, C., Bisnath, A., Manhica, V., 2008. In: Satish-Kumar, M., Motoyoshi, Y., Osani, Y., Hiroi, Y., Shiraishi, K. (Eds.), *Geodynamic evolution of east Antarctica: a key to east–west gondwana connection*. Geological Society, London, Special Publications 308, 91–119.
- Grantham, G.H., Macey, P.H., Horie, K., Kawakami, T., Ishikawa, M., Satish-Kumar, M., Tsuchiya, N., Graser, P., Azavedo, S., in press. Comparison of the metamorphic history of the Monapo Complex, northern Mozambique and Balchenfjella and Austramerian areas, Sør Rondane, Antarctica: implications for the Kuunga Orogeny and the amalgamation of East and West Gondwana. *Precambrian Research*. <http://dx.doi.org/10.1016/j.precamres.2012.11.012>
- Hargrove, U.S., Hanson, R.E., Martin, M.W., Belkinsop, T.G., Bowring, S.A., Walker, N., Munyanyiwa, H., 2003. Tectonic evolution of the Zambezi orogenic belt: geochronological, structural and petrological constraints from northern Zimbabwe. *Precambrian Research* 123, 158–186.
- Holmes, A., 1951. The sequence of pre-Cambrian orogenic belts in south and central Africa. In: 18th International Geological Congress, London, 1948, 14, pp. 254–269.
- Hötlz, S., Hoffmann, A.W., Todt, W., Köhler, H., 1994. U-Pb geochronology of the Sri Lankan basement. *Precambrian Research* 66, 123–149.
- Jacobs, J., Fanning, C.M., Henjes-Kunst, F., Olesch, M., Paech, H.J., 1998. Continuation of the Mozambique Belt into East Antarctica: Grenville age metamorphism and polyphase Pan-African high grade events in central Dronning Maud Land. *Journal of Geology* 106, 385–406.
- Jacobs, J., Bauer, W., Fanning, C.M., 2003. Late Neoproterozoic/early Palaeozoic events in central Dronning Maud Land and significance for the southern extension of the East African Orogen into East Antarctica: *Precambrian Research* 126, 27–53.
- Jacobs, J., Bingen, B., Thomas, R.J., Bauer, W., Wingate, M., Feito, P., 2008. Early Palaeozoic orogenic collapse and voluminous late-tectonic magmatism in Dronning Maud Land and Mozambique: insights into the partially delaminated orogenic root of the East African–Antarctic Orogen? In: Satish-Kumar, M., Motoyoshi, Y., Osani, Y., Hiroi, Y., Shiraishi, K. (Eds.), *Geodynamic Evolution of East Antarctica: A Key to East–West Gondwana Connection*. Geological Society, London, Special Publications 308, pp. 69–90.
- Jacobs, J., Thomas, R.J., 2004. Himalayan-type indenter-escape tectonics model for the southern part of the late Neoproterozoic-early Palaeozoic East African–Antarctic Orogen. *Geology* 32, 721–724.
- Jamal, D.L., 2005. Crustal studies across selected geotransects in NE Mozambique: differentiating between Mozambiquan (~Kibaran) and Pan-African Events, with

- implications for Gondwana Studies. Unpublished PhD thesis. University of Cape Town, South Africa.
- Jöns, N., Schenk, V., 2008. Relics of the Mozambique Ocean in the central East African Orogen: evidence from the Vohibory Block of southern Madagascar. *Journal of Metamorphic Geology* 26, 17–28.
- Jourde, G., Wolff, J.-P., Trotterreau, G., 1974. Géologie et minéralisations de le feuille Nampula. In: BRGM report 74 Moz 007, 54 pp.
- Karlsson, J.P., 2006. An investigation of the felsic Ramiane Pluton in the Monapo structure, northern Moçambique. MSc Thesis. Geological Institute, University of Lund, No. 202, p. 40.
- Kriegsman, L.M., 1995. The Pan-African event in East Antarctica: a view from Sri Lanka and the Mozambique Belt. *Precambrian Research* 75, 263–277.
- Kröner, A., Sacchi, R., Jaeckel, P., Costa, M., 1997. Kibaran magmatism and Pan-African granulite metamorphism in northern Mozambique: single zircon ages and regional implications. *Journal of African Earth Sciences* 25, 467–484.
- Kröner, A., Willner, A.P., Hegner, E., Jaeckel, P., Nemchin, A.A., 2001. Single zircon ages PT evolution and Nd isotopic systematics of high-grade gneisses in southern Malawi and their bearing on the evolution of the Mozambique belt in southeastern Africa. *Precambrian Research* 109, 257–291.
- Lachelt, S., 2004. The geology and mineral resources of Mozambique. Direcção Nacional de Geologia, Mozambique. Council for Geosciences, South Africa, 515 pp.
- Ludwig, K.R., 1999. Isoplot/Ex version 2.00: a geochronological toolkit for Microsoft Excel. Berkeley Geochronology Centre, California, USA, Special Publication 1a, 46 pp.
- Ludwig, K.R., 2000. SQUID 1.00, a user's manual. Berkeley Geochronology Center Special Publication, 2.
- Macey, P.H., Ingram, B.A., Cronwright, M.S., Botha, G.A., Roberts, M.R., Grantham, G.H., Maree, L.P., Botha, P.M.W., Kota, M., Opperman, R., Haddon, I.G., Nolte, J.C., Rower, M., 2007. Map Explanation Sheets Alto Molocué (1537), Murrupula (1538), Nampula (1539), Mogincual (1540), Errego (1637), Gilé (1638), and Angoche (1639–40). National Directorate of Geology, Republic of Mozambique.
- Macey, P.H., Thomas, R.J., Grantham, G.H., + 20 others, 2010. Mesoproterozoic geology of the Nampula Block, northern Mozambique: tracing fragments of Mesoproterozoic crust in the heart of Gondwana. *Precambrian Research* 182, 124–148.
- Meert, J., 2003. A synopsis of events related to the assembly of eastern Gondwana. *Tectonophysics* 362, 1–40.
- Melezhik, V.A., Bingen, B., Fallick, A.E., Gorokhov, I.M., Kuznetsov, A.B., Sandstad, J.S., Solli, A., Bjerkgard, T., Henderson, I.H.C., Boyd, R., Jamal, D., Moniz, A., 2008. Isotope chemostratigraphy of marbles in northeastern Mozambique: apparent depositional ages and tectonostratigraphic implications. *Precambrian Research* 162, 540–558.
- Meschede, M., 1986. A method of discriminating between different types of mid ocean ridge basalts and continental tholeiites with the Nb-Zr-Y diagram. *Chemical Geology* 56, 207–218.
- Muhongo, S., Kröner, A., Nemchin, A.A., 2001. Single zircon evaporation and SHRIMP ages for granulite-facies rocks in the Mozambique Belt of Tanzania. *The Journal of Geology* 109, 171–189.
- Muhongo, S., Lenoir, J.-L., 1994. Pan-African granulite facies metamorphism in the Mozambique belt of Tanzania: U-Pb zircon geochronology. *Journal of the Geological Society London* 151, 343–347.
- Norconsult, 2007a. Mineral Resources Management Capacity Building Project, Republic of Mozambique; Component 2: Geological infrastructure Development Project, Geological Mapping Lot 1; Sheet Explanation: 32 Sheets; Scale: 1/250000, Report No. B6.f, National Directorate of Geology, Republic of Mozambique.
- Norconsult, 2007b. Mineral Resources Management Capacity Building Project, Republic of Mozambique; Component 2: Geological infrastructure Development Project, Geological Mapping Lot 1; Geophysical Interpretation, Report No. B4, National Directorate of Geology, Republic of Mozambique.
- Paces, J.B., Miller, J.D., 1989. Precise U-Pb ages of the Duluth Complex and related mafic intrusions, NE Minnesota: Geochronological insights to physical, petrogenetic, paleomagnetic and tectomagmatic processes associated with the 1.1Ga midcontinent rift. *Journal of Geophysical Research* 98B, 13997–14013.
- Pearce, J.A., Norry, M.J., 1979. Petrographic implications of Ti, Zr, Y and Nb variations in volcanic rocks. *Contributions Mineral Petrology* 69, 33–47.
- Peccerillo, A., Taylor, T.S., 1976. Geochemistry of Eocene calc-alkaline volcanic rocks from Kastamonu area, northern Turkey. *Contributions to Mineralogy and Petrology* 58, 63–81.
- Pinna, P., 1995. On the dual nature of the Mozambique Belt, Mozambique to Kenya. *Journal of African Earth Sciences* 21, 477–480.
- Pinna, P., Marteau, J., 1987. Carta geológica de Moçambique, 1:1,000,000 scale, with explanatory notes. Instituto Nacional de Geologia, Maputo.
- Pinna, P., Jourde, G., Calvez, J.Y., Mroz, J.P., Marques, J.M., 1993. The Mozambique Belt in northern Mozambique: Neoproterozoic (1100–850 Ma) crustal growth and tectogenesis, and superimposed Pan-African (800–550 Ma) tectonism. *Precambrian Research* 62, 1–59.
- Ravikant, V., 2006. Sm–Nd isotopic evidence for late Mesoproterozoic metamorphic relics in the East African Orogen from the Schirmacher Oasis, East Antarctica. *Journal of Geology* 114, 615–625.
- Ravikant, V., Laux, J.H., Pimentel, M., 2008. Sm–Nd and U–Pb isotopic constraints for crustal evolution during the Late Neoproterozoic from rocks of the Schirmacher Oasis, East Antarctica: geodynamic development coeval with the East African Orogeny, US Geological Survey, Open-File Report 2007-1047, Geological Survey and the National Academies USES OF-2007-1047, Short Research Paper 007; <http://dx.doi.org/10.3133/of2007-1047.srp007>
- Rey, P., Vanderhaeghe, O., Teyssier, C., 2001. Gravitational collapse of the continental crust: definition, regimes and modes. *Tectonophysics* 342, 3–4.
- Roberts, M.P., Grantham, G.H., Cronwright, M.S., Sacchi, R., Ingram, B.A., Azevedo, S., Walliser, A., August, R.B., 2005. Preliminary pressure temperature determinations on granulite-facies rocks of the Mugeba Klippe, north central Mozambique. In: Abstract, GEO2005, Durban, South Africa, 4–7 July, p. 84.
- Rubatto, D., 2002. Zircon trace element geochemistry: partitioning with garnet and the link between U–Pb ages and metamorphism. *Chemical Geology* 184, 123–138.
- Sacchi, R., Marques, J.M., Costa, M., Casati, C., 1984. Kibaran events in the southern most Mozambique Belt. *Precambrian Research* 25, 141–159.
- Sacchi, R., Cadoppi, P., Costa, M., 2000. Pan-African reactivation of the Lúrio segment of the Kibaran Belt system: a reappraisal from recent age determinations in northern Mozambique. *Journal of African Earth Sciences* 30, 629–639.
- Sajeev, K., Osanai, Y., Connolly, J.A.D., Suzuki, S., Ishioka, J., Kagami, H., Rino, S., 2007. Extreme crustal metamorphism during a Neoproterozoic event in Sri Lanka: a study of dry mafic granulites. *Journal of Petrology* 115, 563–582.
- Selverstone, J., 2005. Are the Alps collapsing? *Annual Reviews in Earth Sciences* 33, 113–132.
- Siegfried, P.R., 1999. The Monapo structure and intrusive complex – an example of large scale alkaline metasomatism in northern Mozambique. In: Stanley, C.J., Rankin, A.H., Bodnar, R.J., Naden, J., Yardley, B.W.D., Criddle, A.J., Hagni, R.D., Gize, A.P., Pasava, J., Fleet, A.J., Seltmann, R., Halls, C., Stempak, M., Williamson, B., Herrington, R.J., Hill, R.E.T., Prichard, H.M., Wall, F., Williams, C.T., McDonald, I., Wilkinson, J.J., Cooke, D., Cook, N.J., Marshall, B.J., Spry, P., Khin Zaw, L., Meinert, K., Sundblad, P., Scott, S.H.B., Clark, E., Valsamis-Jones, N.J., Beukes, H.J., Stein, J.L., Hannah, F., Neubauer, D.J., Blundell, D.H.M., Alderton, M.P., Smith, S., Mulshaw, R.A., Ixer (Eds.), *Mineral Deposits: Processes to Processing*. Balkema Press, Rotterdam, pp. 683–686, 1468 pp., 2 vols., ISBN 90 5809 068X.
- Stagman, J.G., 1962. The geology of the southern Urungwe District. In: Southern Rhodesia Geological Survey Bulletin No. 55, p. 82.
- Stern, R.J., 2004. Arc assembly and continental collision in the Neoproterozoic East African Orogen: implications for the consolidation of Gondwanaland. *Annual Reviews in Earth and Planetary Sciences* 22, 319–351.
- Thomas, R.J., Jacobs, J., Horstwood, M.S.A., Ueda, K., Bingen, B., Matola, R., 2010. The Mecuburi and Alto Benfica Groups. NE Mozambique: aids to unravelling ca. 1 and 0.5 Ga events in the East African Orogen. *Precambrian Research* 178, 72–90.
- Ueda, K., Jacobs, J., Thomas, R.J., Kosler, J., Jourdan, F., Matola, R., 2012. Delamination-induced late-tectonic deformation and high-grade metamorphism of the Proterozoic Nampula Complex, northern Mozambique. *Precambrian Research* 196–197, 275–294.
- Vail, J.R., Snelling, N.J., 1971. Isotope measurements for the Zambesi orogenic belt and the Urungwe Klippe, Rhodesia. *Geologische Rundschau* 60, 619–630.
- Viola, G., Hendersen, I.H.C., Bingen, B., Thomas, R.J., Smethurst, M.A., de Azavedo, S., 2008. Growth and collapse of a deeply eroded orogen: insights from structural and geochronological constraints on the Pan-African evolution of NE Mozambique. *Tectonics* 27, TC5009, <http://dx.doi.org/10.1029/2008TC002284>.
- Whalen, J.B., Currie, K.L., Chappell, B.W., 1987. A-type granites: geochemical characteristics, discrimination and petrogenesis. *Contributions to Mineralogy and Petrology* 95, 407–419.
- Williams, I.S., 1998. U–Th–Pb Geochronology by Ion Microprobe. In: McKibben, M.A., Shanks III, W.C., Ridley, W.I. (Eds.), *Applications of microanalytical techniques to understanding mineralizing processes*. *Reviews in Economic Geology*, 7, pp. 1–35.